2

NUREG/CR-5651
ORNL/TM-11692

An Investigation of Crack-Tip Stress Field Criteria for Predicting Cleavage-Crack Initiation

Prepared by
J. Keeney-Walker, B. R. Bass, J. D. Landes

Oak Ridge National Laboratory

Prepared for
U.S. Nuclear Regulatory Commission

AVAILABILITY NOTICE

Availability of Reference Materials Cited in NRC Publications

Most documents cited in NRC publications will be available from one of the following sources:

1. The NRC Public Document Room, 2120 L Street, NW., Lower Level, Washington, DC 20555

2. The Superintendent of Documents, U.S. Government Printing Office, P.O. Box 37082, Washington, DC 20013-7082

3. The National Technical Information Service, Springfield, VA 22161

Although the listing that follows represents the majority of documents cited in NRC publications, it is not intended to be exhaustive.

Referenced documents available for inspection and copying for a fee from the NRC Public Document Room include NRC correspondence and internal NRC memoranda; NRC bulletins, circulars, information notices, inspection and investigation notices; licensee event reports; vendor reports and correspondence; Commission papers; and applicant and licensee documents and correspondence.

The following documents in the NUREG series are available for purchase from the GPO Sales Program: formal NRC staff and contractor reports, NRC-sponsored conference proceedings, international agreement reports, grant publications, and NRC booklets and brochures. Also available are regulatory guides, NRC regulations in the *Code of Federal Regulations*, and *Nuclear Regulatory Commission Issuances*.

Documents available from the National Technical Information Service include NUREG-series reports and technical reports prepared by other Federal agencies and reports prepared by the Atomic Energy Commission, forerunner agency to the Nuclear Regulatory Commission.

Documents available from public and special technical libraries include all open literature items, such as books, journal articles, and transactions. *Federal Register* notices, Federal and State legislation, and congressional reports can usually be obtained from these libraries.

Documents such as theses, dissertations, foreign reports and translations, and non-NRC conference proceedings are available for purchase from the organization sponsoring the publication cited.

Single copies of NRC draft reports are available free, to the extent of supply, upon written request to the Office of Administration, Distribution and Mail Services Section, U.S. Nuclear Regulatory Commission, Washington, DC 20555.

Copies of industry codes and standards used in a substantive manner in the NRC regulatory process are maintained at the NRC Library, 7920 Norfolk Avenue, Bethesda, Maryland, for use by the public. Codes and standards are usually copyrighted and may be purchased from the originating organization or, if they are American National Standards, from the American National Standards Institute, 1430 Broadway, New York, NY 10018.

DISCLAIMER NOTICE

NUREG/CR--5651

TI92 000034

An Investigation of Crack-Tip Stress Field Criteria for Predicting Cleavage-Crack Initiation

Manuscript Completed: September 1990
Date Published: September 1991

Prepared by
J. Keeney-Walker, B. R. Bass, J. D. Landes

Oak Ridge National Laboratory
Operated by Martin Marietta Energy Systems, Inc.

Oak Ridge National Laboratory
Oak Ridge, TN 37831-6285

Prepared for
Division of Engineering
Office of Nuclear Regulatory Research
U.S. Nuclear Regulatory Commission
Washington, DC 20555
NRC FIN B0119
Under Contract No. DE-AC05-84OR21400

ABSTRACT

Cleavage-crack initiation in large-scale wide-plate (WP) specimens could not be accurately predicted from small, compact (CT) specimens by using a linear-elastic fracture-mechanics, K_{Ic}, methodology. In the wide-plate tests conducted by the Heavy-Section Steel Technology Program at Oak Ridge National Laboratory, crack initiation has consistently occurred at stress-intensity (K_I) values ranging from two to four times those predicted by the CT specimens. Studies were initiated to develop crack-tip stress field criteria incorporating effects of geometry, size, and constraint that will lead to improved predictions of cleavage initiation in WP specimens from CT specimens. The work centers around nonlinear two- and three-dimensional finite-element analyses of the crack-tip stress fields in these geometries. Analyses were conducted on CT and WP specimens for which cleavage initiation fracture had been measured in laboratory tests. The local crack-tip fields generated for these specimens were then used in the evaluation of fracture correlation parameters to augment the K_I parameter for predicting cleavage initiation. Parameters of hydrostatic constraint and of maximum principal stress, measured volumetrically, are included in these evaluations. The results suggest that the cleavage initiation process can be correlated with the local crack-tip fields via a maximum principal stress criterion based on achieving a critical area within a critical stress contour. This criterion has been successfully applied to correlate cleavage initiation in 2T-CT and WP specimen geometries.

CONTENTS

LIST OF FIGURES

LIST OF TABLES

FOREWORD

The work reported here was performed at Oak Ridge National Laboratory under the Heavy-Section Steel Technology (HSST) Program, W. E. Pennell, Program Manager. The program is sponsored by the Office of Nuclear Regulatory Research of the U.S. Nuclear Regulatory Commission (NRC). The technical monitor for the NRC is M. E. Mayfield.

This report is designated HSST Report 109. Prior and future reports in this series are listed below.

1. S. Yukawa, General Electric Company, Schenectady, N.Y., *Evaluation of Periodic Proof Testing and Warm Prestressing Procedures for Nuclear Reactor Vessels*, HSSTP-TR-1, July 1, 1969.
2. L. W. Loechel, Martin Marietta Corporation, Denver, Colo., *The Effect of Testing Variables on the Transition Temperature in Steel*, MCR-69-189, November 20, 1969.
3. P. N. Randall, TRW Systems Group, Redondo Beach, Calif., *Gross Strain Measure of Fracture Toughness of Steels*, HSSTP-TR-3, November 1, 1969.
4. C. Visser, S. E. Gabrielse, and W. VanBuren, Westinghouse Electric Corporation, PWR Systems Division, Pittsburgh, Pa., *A Two-Dimensional Elastic-Plastic Analysis of Fracture Test Specimens*, WCAP-7368, October 1969.
5. T. R. Mager and F. O. Thomas, Westinghouse Electric Corporation, PWR Systems Division, Pittsburgh, Pa., *Evaluation* by *Linear Elastic Fracture Mechanics of Radiation Damage to Pressure Vessel Steels*, WCAP-7328 (Rev.), October 1969.
6. W. O. Shabbits, W. H. Pryle, and E. T. Wessel, Westinghouse Electric Corporation, PWR Systems Division, Pittsburgh, Pa., *Heavy-Section Fracture Toughness Properties of A533 Grade B Class 1 Steel Plate and Submerged Arc Weldment*, WCAP-7414, December 1969.
7. F. J. Loss, Naval Research Laboratory, Washington, D.C., *Dynamic Tear Test Investigations of the Fracture Toughness of Thick-Section Steel*, NRL-7056, May 14, 1970.
8. P. B. Crosley and E. J. Ripling, Materials Research Laboratory, Inc., Glenwood, Ill., *Crack Arrest Fracture Toughness of A533 Grade B Class 1 Pressure Vessel Steel*, HSSTP-TR-8, March 1970.
9. T. R. Mager, Westinghouse Electric Corporation, PWR Systems Division, Pittsburgh, Pa., *Post-Irradiation Testing* of *2T Compact Tension Specimens*, WCAP-7561, August 1970.
10. T. R. Mager, Westinghouse Electric Corporation, PWR Systems Division, Pittsburgh, Pa., *Fracture Toughness Characterization Study of A533, Grade B, Class 1 Steel*, WCAP-7578, October 1970.
11. T. R. Mager, Westinghouse Electric Corporation, PWR Systems Division, Pittsburgh, Pa., *Notch Preparation in Compact Tension Specimens*, WCAP-7579, November 1970.

12. N. Levy and P. V. Marcal, Brown University, Providence, R.I., *Three-Dimensional Elastic-Plastic Stress and Strain Analysis for Fracture Mechanics, Phase I: Simple Flawed Specimens,* HSSTP-TR-12, December 1970.

13. W. O. Shabbits, Westinghouse Electric Corporation, PWR Systems Division, Pittsburgh, Pa., *Dynamic Fracture Toughness Properties of Heavy Section A533 Grade B Class 1 Steel Plate,* WCAP-7623, December 1970.

14. P. N. Randall, TRW Systems Group, Redondo Beach, Calif., *Gross Strain Crack Tolerance of A 533-B Steel,* HSSTP-TR-14, May 1, 1971.

15. H. T. Corten and R. H. Sailors, University of Illinois, Urbana, Ill., *Relationship Between Material Fracture Toughness Using Fracture Mechanics and Transition Temperature Tests,* T&AM Report 346, August 1, 1971.

16. T. R. Mager and V. J. McLaughlin, Westinghouse Electric Corporation, PWR Systems Division, Pittsburgh, Pa., *The Effect of an Environment of High Temperature Primary Grade Nuclear Reactor Water on the Fatigue Crack Growth Characteristics of A533 Grade B Class 1 Plate and Weldment Material,* WCAP-7776, October 1971.

17. N. Levy and P. V. Marcal, Brown University, Providence, R.I., *Three-Dimensional Elastic-Plastic Stress and Strain Analysis for Fracture Mechanics, Phase II: Improved Modelling,* HSSTP-TR-17, November 1971.

18. S. C. Grigory, Southwest Research Institute, San Antonio, Tex., *Tests of 6-in.-Thick Flawed Tensile Specimens, First Technical Summary Report, Longitudinal Specimens Numbers I through 7,* HSSTP-TR-18, June 1972.

19. P. N. Randall, TRW Systems Group, Redondo Beach, Calif., *Effects of Strain Gradients on the Gross Strain Crack Tolerance of A533-B Steel,* HSSTP-TR-19, June 15, 1972.

20. S. C. Grigory, Southwest Research Institute, San Antonio, Tex., *Tests of 6-Inch-Thick Flawed Tensile Specimens, Second Technical Summary Report, Transverse Specimens Numbers 8 through 10, Welded Specimens Numbers 11 through 13,* HSSTP-TR-20, June 1972.

21. L. A. James and J. A. Williams, Hanford Engineering Development Laboratory, Richland, Wash., Heavy Section Steel Technology Program Technical Report No. 21, *The Effect of Temperature and Neutron Irradiation Upon the Fatigue-Crack Propagation Behavior of ASTM A533 Grade B, Class 1 Steel,* HEDL-TME 72-132, September 1972.

22. S. C. Grigory, Southwest Research Institute, San Antonio, Tex., *Tests of 6-Inch-Thick Flawed Tensile Specimens, Third Technical Summary Report, Longitudinal Specimens Numbers 14 through 16, Unflawed Specimen Number 17,* HSSTP-TR-22, October 1972.

23. S. C. Grigory, Southwest Research Institute, San Antonio, Tex., *Tests of 6-Inch-Thick Tensile Specimens, Fourth Technical Summary Report, Tests of 1-Inch-Thick Flawed Tensile Specimens for Size Effect Evaluation,* HSSTP-TR-23, June 1973.

24. S. P. Ying and S. C. Grigory, Southwest Research Institute, San Antonio, Tex., *Tests of 6-Inch-Thick Tensile Specimens, Fifth Technical Summary Report, Acoustic Emission Monitoring of One-Inch and Six-Inch-Thick Tensile Specimens,* HSSTP-TR-24, November 1972.

25. R. W. Derby, J. G. Merkle, G. C. Robinson, G. D. Whitman, and F. J. Witt, Oak Ridge Natl. Lab., Oak Ridge, Tenn., *Test of 6-Inch-Thick Pressure Vessels. Series 1: Intermediate Test Vessels V-1 and V-2,* ORNL-4895, February 1974.

26. W. J. Stelzman and R. G. Berggren, Oak Ridge Natl. Lab., Oak Ridge, Tenn., *Radiation Strengthening and Embrittlement in Heavy Section Steel Plates and Welds,* ORNL-4871, June 1973.

27. P. B. Crosley and E. J. Ripling, Materials Research Laboratory, Inc., Glenwood, Ill., *Crack Arrest in an Increasing K-Field,* HSSTP-TR-27, January 1973.

28. P. V. Marcal, P. M. Stuart, and R. S. Bettes, Brown University, Providence, R.I., *Elastic Plastic Behavior of a Longitudinal Semi-Elliptic Crack in a Thick Pressure Vessel,* HSSTP-TR-28, June 1973.

29. W. J. Stelzman, R. G. Berggren, and T. N. Jones, Oak Ridge Natl. Lab., Oak Ridge, Tenn., *ORNL Characterization of Heavy-Section Steel Technology Program Plates 01, 02 and 03,* USNRC Report NUREG/CR-4092 (ORNL/TM-9491), April 1985.

30. Canceled.

31. J. A. Williams, Hanford Engineering Development Laboratory, Richland, Wash., *The Irradiation and Temperature Dependence of Tensile and Fracture Properties of ASTM A533, Grade B, Class 1 Steel Plate and Weldment,* HEDL-TME 73-75, August 1973.

32. J. M. Steichen and J. A. Williams, Hanford Engineering Development Laboratory, Richland, Wash., *High Strain Rate Tensile Properties of Irradiated ASTM A533 Grade B Class 1 Pressure Vessel Steel,* July 1973.

33. P. C. Riccardella and J. L. Swedlow, Westinghouse Electric Corporation, Pittsburgh, Pa., *A Combined Analytical-Experimental Fracture Study of the Two Leading Theories of Elastic-Plastic Fracture (J-Integral and Equivalent Energy),* WCAP-8224, October 1973.

34. R. J. Podlasek and R. J. Eiber, Battelle Columbus Laboratories, Columbus, Ohio, *Final Report on Investigation of Mode III Crack Extension in Reactor Piping*, December 14, 1973.

35. T. R. Mager, J. D. Landes, D. M. Moon, and V. J. McLaughlin, Westinghouse Electric Corporation, Pittsburgh, Pa., *Interim Report on the Effect of Low Frequencies on the Fatigue Crack Growth Characteristics of A533 Grade B Class 1 Plate in an Environment of High-Temperature Primary Grade Nuclear Reactor Water,* WCAP-8256, December 1973.

36. J. A. Williams, Hanford Engineering Development Laboratory, Richland, Wash., *The Irradiated Fracture Toughness of ASTM A533, Grade B, Class 1 Steel Measured with a Four-Inch-Thick Compact Tension Specimen,* HEDL-TME 75-10, January 1975.

37. R. H. Bryan, J. G. Merkle, M. N. Raftenberg, G. C. Robinson, and J. E. Smith, Oak Ridge Natl. Lab., Oak Ridge, Tenn., *Test of 6-Inch-Thick Pressure Vessels. Series 2: Intermediate Test Vessels V-3, V-4, and V-6*, ORNL-5059, November 1975.

38. T. R. Mager, S. E. Yanichko, and L. R. Singer, Westinghouse Electric Corporation, Pittsburgh, Pa., *Fracture Toughness Characterization of HSST Intermediate Pressure Vessel Material*, WCAP-8456, December 1974.

39. J. G. Merkle, G. D. Whitman, and R. H. Bryan, Oak Ridge Natl. Lab., Oak Ridge, Tenn., *An Evaluation* of *the HSST Program Intermediate Pressure Vessel Tests in Terms* of *Light-Water-Reactor Pressure Vessel Safety*, ORNL/TM-5090, November 1975.

40. J. C. Merkle, G. C. Robinson, P. P. Holz, J. E. Smith, and R. H. Bryan, Oak Ridge Natl. Lab., Oak Ridge, Tenn., *Test of 6-In.-Thick Pressure Vessels. Series 3: Intermediate Test Vessel V-7*, USNRC Report ORNL/NUREG-1, August 1976.

41. J. A. Davidson, L. J. Ceschini, R. P. Shogan, and G. V. Rao, Westinghouse Electric Corporation, Pittsburgh, Pa., *The Irradiated Dynamic Fracture Toughness* of *ASTM A533, Grade B, Class 1 Steel Plate and Submerged Arc Weldment*, WCAP-8775, October 1976.

42. R. D. Cheverton, Oak Ridge Natl. Lab., Oak Ridge, Tenn., *Pressure Vessel Fracture Studies Pertaining to a PWR LOCA-ECC Thermal Shock: Experiments TSE-1 and TSE-2*, USNRC Report ORNL/NUREG/TM-31, September 1976.

43. J. G. Merkle, G. C. Robinson, P. P. Holz, and J. E. Smith, Oak Ridge Natl. Lab., Oak Ridge, Tenn., *Test of 6-In.-Thick Pressure Vessels. Series 4: Intermediate Test Vessels V-5 and V-9 with Inside Nozzle Corner Cracks*, USNRC Report ORNL/NUREG-7, August 1977.

44. J. A. Williams, Hanford Engineering Development Laboratory, Richland, Wash., *The Ductile Fracture Toughness of Heavy Section Steel Plate*, USNRC Report NUREG/CR-0859, September 1979.

45. R. H. Bryan, T. M. Cate, P. P. Holz, T. A. King, J. G. Merkle, C. C. Robinson, G. C. Smith, J. E. Smith, and G. D. Whitman, Oak Ridge Natl. Lab., Oak Ridge, Tenn., *Test of 6-in.-Thick Pressure Vessels. Series 3: Intermediate Test Vessel V-7A Under Sustained Loading*, USNRC Report ORNL/NUREG-9, February 1978.

46. R. D. Cheverton and S. E. Bolt, Oak Ridge Natl. Lab., Oak Ridge, Tenn., *Pressure Vessel Fracture Studies Pertaining to a PWR LOCA-ECC Thermal Shock: Experiments TSE-3 and TSE-4 and Update of TSE-1 and TSE-2 Analysis*, USNRC Report ORNL/NUREG-22, December 1977.

47. D. A. Canonico, Oak Ridge Natl. Lab., Oak Ridge, Tenn., *Significance of Reheat Cracks to the Integrity of Pressure Vessels for Light-Water Reactors*, USNRC Report ORNL/NUREG-15, July 1977.

48. G. C. Smith and P. P. Holz, Oak Ridge Natl. Lab., Oak Ridge, Tenn., *Repair Weld Induced Residual Stresses in Thick-Walled Steel Pressure Vessels*, USNRC Report NUREG/CR-0093 (ORNL/NUREG/TM-153), June 1978.

49. P. P. Holz and S. W. Wismer, Oak Ridge Natl. Lab., Oak Ridge, Tenn., *Half-Bead (Temper) Repair Welding for HSST Vessels,* USNRC Report NUREG/CR-0113 (ORNL/NUREG/TM-177), June 1978.

50. G. C. Smith, P. P. Holz, and W. J. Stelzman, Oak Ridge Natl. Lab., Oak Ridge, Tenn., *Crack Extension and Arrest Tests of Axially Flawed Steel Model Pressure Vessels,* USNRC Report NUREG/CR-0126 (ORNL/NUREG/TM-196), October 1978.

51. R. H. Bryan, P. P. Holz, J. G. Merkle, G. C. Smith, J. E. Smith, and W. J. Stelzman, Oak Ridge Natl. Lab., Oak Ridge, Tenn., *Test of 6-in.-Thick Pressure Vessels. Series 3: Intermediate Test Vessel V-7B,* USNRC Report NUREG/CR-0309 (ORNL/NUREG-38), October 1978.

52. R. D. Cheverton, S. K. Iskander, and S. E. Bolt, Oak Ridge Natl. Lab., Oak Ridge, Tenn., *Applicability of LEFM to the Analysis of PWR Vessels Under LOCA-ECC Thermal Shock Conditions,* USNRC Report NUREG/CR-0107 (ORNL/NUREG-40), October 1978.

53. R. H. Bryan, D. A. Canonico, P. P. Holz, S. K. Iskander, J. G. Merkle, J. E. Smith, and W. J. Stelzman, Oak Ridge Natl. Lab., Oak Ridge, Tenn., *Test of 6-in.-Thick Pressure Vessels, Series 3: Intermediate Test Vessel V-8,* USNRC Report NUREG/CR-0675 (ORNL/ NUREG-58), December 1979.

54. R. D. Cheverton and S. K. Iskander, Oak Ridge Natl. Lab., Oak Ridge, Tenn., *Application of Static and Dynamic Crack Arrest Theory to TSE-4,* USNRC Report NUREG/CR-0767 (ORNL/NUREG-57), June 1979.

55. J. A. Williams, Hanford Engineering Development Laboratory, Richland, Wash., *Tensile Properties of Irradiated and Unirradiated Welds of A533 Steel Plate and A508 Forgings,* USNRC Report NUREG/CR-1158 (ORNL/Sub/79-50917/2), July 1979.

56. K. W. Carlson and J. A. Williams, Hanford Engineering Development Laboratory, Richland, Wash., *The Effect of Crack Length and Side Grooves on the Ductile Fracture Toughness Properties of ASTM A533 Steel,* USNRC Report NUREG/CR-1171 (ORNL/Sub/79-50917/3), October 1979.

57. P. P. Holz, Oak Ridge Natl. Lab., Oak Ridge, Tenn., *Flaw Preparations for HSST Program Vessel Fracture Mechanics Testing; Mechanical-Cyclic Pumping and Electron-Beam Weld-Hydrogen Charge Cracking Schemes,* USNRC Report NUREG/CR-1274 (ORNL/NUREG/TM-369), May 1980.

58. S. K. Iskander, Computer Sciences Div., Union Carbide Corp. Nuclear Div., Oak Ridge, Tenn., *Two Finite Element Techniques for Computing Mode I Stress Intensity Factors in Two- or Three-Dimensional Problems,* USNRC Report NUREG/CR-1499 (ORNL/NUREG/CSD/TM-14), February 1981.

59. P. B. Crosley and E. J. Ripling, Materials Research Laboratory, Glenwood, Ill., *Development of a Standard Test for Measuring K_{Ia} with a Modified Compact Specimen,* USNRC Report NUREG/CR-2294 (ORNL/Sub/81-7755/1), August 1981.

60. S. N. Atluri, B. R. Bass, J. W. Bryson, and K. Kathiresan, Computer Sciences Div., Oak Ridge Gaseous Diffusion Plant, Oak Ridge, Tenn., *NOZ-FLAW: A Finite Element*

Program for Direct Evaluation of Stress Intensity Factors for Pressure Vessel Nozzle-Corner Flaws, USNRC Report NUREG/CR-1843 (ORNL/NUREG/CSD/TM-18), March 1981.

61. A. Shukla, W. L. Fourney, and G. R. Irwin, University of Maryland, College Park, Md., *Study of Energy Loss and Its Mechanisms in Homalite 100 During Crack Propagation and Arrest*, USNRC Report NUREG/CR-2150 (ORNL/Sub/79-7778/1), August 1981.

62. S. K. Iskander, R. D. Cheverton, and D. G. Ball, Oak Ridge Natl. Lab., Oak Ridge, Tenn., *OCA-I, A Code for Calculating the Behavior of Flaws on the Inner Surface of a Pressure Vessel Subjected to Temperature and Pressure Transients*, USNRC Report NUREG/CR-2113 (ORNL/NUREG-84), August 1981.

63. R. J. Sanford, R. Chona, W. L. Fourney, and G. R. Irwin, University of Maryland, College Park, Md., *A Photoelastic Study of the Influence of Non-Singular Stresses in Fracture Test Specimens*, USNRC Report NUREG/CR-2179 (ORNL/Sub/79-7778/2), August 1981.

64. B. R. Bass, S. N. Atluri, J. W. Bryson, and K. Kathiresan, Oak Ridge Natl. Lab., Oak Ridge, Tenn., *OR-FLAW: A Finite Element Program for Direct Evaluation of K-Factors for User-Defined Flaws in Plate, Cylinders, and Pressure-Vessel Nozzle Corners*, USNRC Report NUREG/CR-2494 (ORNL/CSD/TM-165), April 1982.

65. B. R. Bass and J. W. Bryson, Oak Ridge Natl. Lab., Oak Ridge Tenn., *ORMGEN-3D: A Finite Element Mesh Generator for 3-Dimensional Crack Geometries*, USNRC Report NUREG/CR-2997, Vol. 1 (ORNL/TM-8527/V1), December 1982.

66. B. R. Bass and J. W. Bryson, Oak Ridge Natl. Lab., Oak Ridge, Tenn., *ORVIRT: A Finite Element Program for Energy Release Rate Calculations for 2-Dimensional and 3-Dimensional Crack Models*, USNRC Report NUREG/CR-2997, Vol. 2 (ORNL/TM-8527/V2), February 1983.

67. R. D. Cheverton, S. K. Iskander, and D. G. Ball, Oak Ridge Natl. Lab., Oak Ridge, Tenn., *PWR Pressure Vessel Integrity During Overcooling Accidents: A Parametric Analysis*, USNRC Report NUREG/CR-2895 (ORNL/TM-7931), February 1983.

68. D. G. Ball, R. D. Cheverton, J. B. Drake, and S. K. Iskander, Oak Ridge Natl. Lab., Oak Ridge, Tenn., *OCA-II, A Code for Calculating Behavior of 2-D and 3-D Surface Flaws in a Pressure Vessel Subjected to Temperature and Pressure Transients*, USNRC Report NUREG/ CR-3491 (ORNL-5934), February 1984.

69. A. Sauter, R. D. Cheverton, and S. K. Iskander, Oak Ridge Natl. Lab., Oak Ridge, Tenn., *Modification of OCA-I for Application to a Reactor Pressure Vessel with Cladding on the Inner Surface*, USNRC Report NUREG/CR-3155 (ORNL/TM-8649), May 1983.

70. R. D. Cheverton and D. G. Ball, Martin Marietta Energy Systems, Inc., Oak Ridge Natl. Lab., Oak Ridge, Tenn., *OCA-P, A Deterministic and Probabilistic Fracture-Mechanics Code for Application to Pressure Vessels*, USNRC Report NUREG/CR-3618 (ORNL-5991), May 1984.

71. J. G. Merkle, Martin Marietta Energy Systems, Inc., Oak Ridge Natl. Lab., Oak Ridge, Tenn., *An Examination of the Size Effects and Data Scatter Observed in Small Specimen*

Cleavage Fracture Toughness Testing, USNRC Report NUREG/CR-3672 (ORNL/TM-9088), April 1984.

72. C. E. Pugh et al., Martin Marietta Energy Systems, Inc., Oak Ridge Natl. Lab., Oak Ridge, Tenn., *Heavy-Section Steel Technology Program—Five-Year Plan FY 1983–1987*, USNRC Report NUREG/CR-3595 (ORNL/TM-9008), April 1984.

73. D. G. Ball, B. R. Bass, J. W. Bryson, R. D. Cheverton, and J. B. Drake, Martin Marietta Energy Systems, Inc., Oak Ridge Natl. Lab., Oak Ridge, Tenn., *Stress Intensity Factor Influence Coefficients for Surface Flaws in Pressure Vessels*, USNRC Report NUREG/CR-3723 (ORNL/CSD/TM-216), February 1985.

74. W. R. Corwin, R. G. Berggren, and R. K. Nanstad, Martin Marietta Energy Systems, Inc., Oak Ridge Natl. Lab., Oak Ridge, Tenn., *Charpy Toughness and Tensile Properties of Neutron Irradiated Stainless Steel Submerged-Arc Weld Cladding Overlay*, USNRC Report NUREG/CR-3927 (ORNL/TM-9309), September 1984.

75. C. W. Schwartz, R. Chona, W. L. Fourney, and G. R. Irwin, University of Maryland, College Park, Md., *SAMCR: A Two-Dimensional Dynamic Finite Element Code for the Stress Analysis of Moving CRacks*, USNRC Report NUREG/CR-3891 (ORNL/Sub/79-7778/3), November 1984.

76. W. R. Corwin, G. C. Robinson, R. K. Nanstad, J. G. Merkle, R. G. Berggren, G. M. Goodwin, R. L. Swain, and T. D. Owings, Martin Marietta Energy Systems, Inc., Oak Ridge Natl. Lab., Oak Ridge, Tenn., *Effects of Stainless Steel Weld Overlay Cladding on the Structural Integrity of Flawed Steel Plates in Bending, Series 1*, USNRC Report NUREG/CR-4015 (ORNL/TM-9390), April 1985.

77. R. H. Bryan, B. R. Bass, S. E. Bolt, J. W. Bryson, D. P. Edmonds, R. W. McCulloch, J. G. Merkle, R. K. Nanstad, G. C. Robinson, K. R. Thoms, and G. D. Whitman, Martin Marietta Energy Systems, Inc., Oak Ridge Natl. Lab., Oak Ridge, Tenn., *Pressurized-Thermal-Shock Test of 6-in.-Thick Pressure Vessels. PTSE-1: Investigation of Warm Prestressing and Upper-Shelf Arrest*, USNRC Report NUREG/CR-4106 (ORNL-6135), April 1985.

78. R. D. Cheverton, D. G. Ball, S. E. Bolt, S. K. Iskander, and R. K. Nanstad, Martin Marietta Energy Systems, Inc., Oak Ridge Natl. Lab., Oak Ridge, Tenn., *Pressure Vessel Fracture Studies Pertaining to the PWR Thermal-Shock Issue: Experiments TSE-5, TSE-5A, and TSE-6*, USNRC Report NUREG/CR-4249 (ORNL-6163), June 1985.

79. R. D. Cheverton, D. G. Ball, S. E. Bolt, S. K. Iskander, and R. K. Nanstad, Martin Marietta Energy Systems, Inc., Oak Ridge Natl. Lab., Oak Ridge, Tenn., *Pressure Vessel Fracture Studies Pertaining to the PWR Thermal-Shock Issue: Experiment TSE-7*, USNRC Report NUREG/CR-4304 (ORNL-6177), August 1985.

80. R. H. Bryan, B. R. Bass, S. E. Bolt, J. W. Bryson, J. G. Merkle, R. K. Nanstad, and G. C. Robinson, Martin Marietta Energy Systems, Inc., Oak Ridge Natl. Lab., Oak Ridge, Tenn., *Test of 6-in.-Thick Pressure Vessels. Series 3: Intermediate Test Vessel V-8A—Tearing Behavior of Low Upper-Shelf Material*, USNRC Report NUREG/CR-4760 (ORNL-6187), May 1987.

81. R. D. Cheverton and D. G. Ball, Martin Marietta Energy Systems, Inc., Oak Ridge Natl. Lab., Oak Ridge, Tenn., *A Parametric Study of PWR Pressure Vessel Integrity During Overcooling Accidents, Considering Both 2-D and 3-D Flaws,* USNRC Report NUREG/CR-4325 (ORNL/TM-9682), August 1985.

82. E. C. Rodabaugh, E. C. Rodabaugh Associates, Inc., Hilliard, Ohio, *Comments on the Leak-Before-Break Concept for Nuclear Power Plant Piping Systems,* USNRC Report NUREG/CR-4305 (ORNL/Sub/82-22252/3), August 1985.

83. J. W. Bryson, Martin Marietta Energy Systems, Inc., Oak Ridge Natl. Lab., Oak Ridge, Tenn., *ORVIRT.PC: A 2-D Finite Element Fracture Analysis Program for a Microcomputer,* USNRC Report NUREG/CR-4367 (ORNL-6208), October 1985.

84. D. G. Ball and R. D. Cheverton, Martin Marietta Energy Systems, Inc., Oak Ridge Natl. Lab., Oak Ridge, Tenn., *Adaptation of OCA-P, A Probabilistic Fracture-Mechanics Code, to a Personal Computer,* USNRC Report NUREG/CR-4468 (ORNL/CSD/TM-233), January 1986.

85. J. W. Bryson and B. R. Bass, Martin Marietta Energy Systems, Inc., Oak Ridge Natl. Lab., Oak Ridge, Tenn., *ORMGEN*.PC: *A Microcomputer Program for Automatic Mesh Generation of 2-D Crack Geometries,* USNRC Report NUREG/CR-4475 (ORNL-6250), March 1986.

86. G. D. Whitman, Martin Marietta Energy Systems, Inc., Oak Ridge Natl. Lab., Oak Ridge, Tenn., *Historical Summary of the Heavy-Section Steel Technology Program and Some Related Activities in Light-Water Reactor Pressure Vessel Safety Research,* USNRC Report NUREG/CR-4489 (ORNL-6259), March 1986.

87. C. Inversini and J. W. Bryson, Martin Marietta Energy Systems, Inc., Oak Ridge Natl. Lab., Oak Ridge, Tenn., *ORPLOT PC: A Graphic Utility for ORMGEN.PC and ORVIRT.PC,* USNRC Report NUREG/CR-4633 (ORNL-6291), June 1986.

88. J. J. McGowan, R. K. Nanstad, and K. R. Thoms, Martin Marietta Energy Systems, Inc., Oak Ridge Natl. Lab., Oak Ridge, Tenn., *Characterization of Irradiated Current-Practice Welds and A533 Grade B Class 1 Plate for Nuclear Pressure Vessel Service,* USNRC Report NUREG/CR-4880 (ORNL/TM-10387), July 1988.

89. K. V. Cook and R. W. McClung, Martin Marietta Energy Systems, Inc., Oak Ridge Natl. Lab., Oak Ridge, Tenn., *Flaw Density Examinations of a Clad Boiling Water Reactor Pressure Vessel Segment,* USNRC Report NUREG/CR-4860 (ORNL/TM-10364), April 1987.

90. D. J. Naus, B. R. Bass, C. E. Pugh, R. K. Nanstad, J. G. Merkle, W. R. Corwin, and G. C. Robinson, Martin Marietta Energy Systems, Inc., Oak Ridge Natl. Lab., Oak Ridge, Tenn., *Crack-Arrest Behavior in SEN Wide Plates of Quenched and Tempered A 533 Grade B Steel Tested Under Nonisothermal Conditions,* USNRC Report NUREG/CR-4930 (ORNL-6388), August 1987.

91. D. B. Barker, R. Chona, W. L. Fourney, and G. R. Irwin, University of Maryland, College Park, Md., *A Report on the Round Robin Program Conducted to Evaluate the Proposed ASTM Standard Test Method for Determining the Plane Strain Crack Arrest*

Fracture Toughness, K_{Ia}, of Ferritic Materials, USNRC Report NUREG/CR-4966 (ORNL/Sub/79-7778/4), January 1988.

92. W. H. Bamford, Westinghouse Electric Corporation, Pittsburgh, Pa., *A Summary of Environmentally Assisted Crack-Growth Studies Performed at Westinghouse Electric Corporation Under Funding from the Heavy-Section Steel Technology Program*, USNRC Report NUREG/CR-5020 (ORNL/Sub/82-21598/1), May 1988.

93. R. H. Bryan, B. R. Bass, S. E. Bolt, J. W. Bryson, W. R. Corwin, J. G. Merkle, R. K. Nanstad, and G. C. Robinson, Martin Marietta Energy Systems, Inc., Oak Ridge Natl. Lab., Oak Ridge, Tenn., *Pressurized-Thermal-Shock Test of 6-in.-Thick Pressure Vessels. PTSE-2: Investigation of Low Tearing Resistance and Warm Prestressing*, USNRC Report NUREG/CR-4888 (ORNL-6377), December 1987.

94. J. H. Giovanola and R. W. Klopp, SRI International, Menlo Park, Calif., *Viscoplastic Stress-Strain Characterization of A533B Class 1 Steel*, USNRC Report NUREG/CR-5066 (ORNL/Sub/87-SA193/1), September 1989.

95. L. F. Miller et al., Martin Marietta Energy Systems, Inc., Oak Ridge Natl. Lab., Oak Ridge, Tenn., *Neutron Exposure Parameters for the Metallurgical Test Specimens in the Fifth Heavy-Section Steel Technology Irradiation Series Capsules*, USNRC Report NUREG/ CR-5019 (ORNL/TM-10582), March 1988.

96. Canceled.

97. D. J. Naus, J. Keeney-Walker, and B. R. Bass, Martin Marietta Energy Systems, Inc., Oak Ridge Natl. Lab., Oak Ridge, Tenn., *High-Temperature Crack-Arrest Behavior in 152-mm-Thick SEN Wide Plates of Quenched and Tempered A 533 Grade B Steel*, USNRC Report NUREG/CR-5330 (ORNL/TM-11083), April 1989.

98. K. V. Cook, R. A. Cunningham, Jr., and R. W. McClung, Martin Marietta Energy Systems, Inc., Oak Ridge Natl. Lab., Oak Ridge, Tenn., *Detection and Characterization of Indications in Segments of Reactor Pressure Vessels*, USNRC Report NUREG/CR-5322 (ORNL/TM-11072), August 1989.

99. R. D. Cheverton, W. E. Pennell, G. C. Robinson, and R. K. Nanstad, Martin Marietta Energy Systems, Inc., Oak Ridge Natl. Lab., Oak Ridge, Tenn., *Impact of Radiation Embrittlement on Integrity of Pressure Vessel Supports for Two PWR Plants*, NUREG/CR-5320 (ORNL/TM-10966), February 1989.

100. D. J. Naus, J. Keeney-Walker, B. R. Bass, S. K. Iskander, R. J. Fields, R. deWitt, and S. R. Low III, Martin Marietta Energy Systems, Inc., Oak Ridge Natl. Lab., Oak Ridge, Tenn., *SEN Wide-Plate Crack-Arrest Tests* Utilizing *A 533 Grade B Class 1 Material: WP-CE Test Series*, USNRC Report NUREG/CR-5408 (ORNL/TM-11269), November 1989.

101. D. J. Naus, J. Keeney-Walker, B. R. Bass, S. K. Iskander, R. J. Fields, R. deWitt, and S. R. Low III, Martin Marietta Energy Systems, Inc., Oak Ridge Natl. Lab., Oak Ridge, Tenn., *High Temperature Crack-Arrest Tests Using 152-mm-Thick SEN Wide Plates of Low Upper-Shelf Base Material: Tests WP-2.2 and WP-2.6*, USNRC Report NUREG/CR-5450 (ORNL/TM-11352), February 1990.

102. Canceled.

103. D. J. Naus, J. Keeney-Walker, B. R. Bass, G. C. Robinson, S. K. Iskander, D. J. Alexander, R. J. Fields, R. deWitt, S. R. Low, C. W. Schwartz, and I.-B. Johansson, Martin Marietta Energy Systems, Inc., Oak Ridge Natl. Lab., Oak Ridge, Tenn., *Crack-Arrest Behavior in SEN Wide Plates of Low Upper-Shelf Base Metal Tested Under Nonisothermal Conditions: WP-2 Series*, USNRC Report NUREG/CR-5451 (ORNL-6584), August 1990.

104. T. L. Dickson, R. D. Cheverton, and D. K. Shum, Martin Marietta Energy Systems, Inc., Oak Ridge Natl. Lab., Oak Ridge, Tenn., *Inclusion of Unstable Ductile Tearing and Extrapolated Crack-Arrest Toughness Data in PWR Vessel Integrity Assessment*, USNRC Report NUREG/CR-5473 (ORNL/TM-11450), May 1990.

105. T. J. Theiss, Martin Marietta Energy Systems, Inc., Oak Ridge Natl. Lab., Oak Ridge, Tenn., *Recommendations for the Shallow-Crack Fracture Toughness Testing Task Within the HSST Program*, USNRC Report NUREG/CR-5554 (ORNL/TM-11509), September 1990.

106. J. G. Merkle, Martin Marietta Energy Systems, Inc., Oak Ridge Natl. Lab., Oak Ridge, Tenn., *An Overview of the Low Upper Shelf Toughness Safety Margin Issue*, USNRC Report NUREG/CR-5552 (ORNL/TM-11314), August 6, 1990.

107. D. K. M. Shum, J. G. Merkle, J. Keeney-Walker, and B. R. Bass, Martin Marietta Energy Systems, Inc., Oak Ridge Natl. Lab., Oak Ridge, Tenn., *Analytical Studies of Transverse Strain Effects on Fracture Toughness for Circumferentially Oriented Cracks*, USNRC Report NUREG/CR-5592 (ORNL/TM-11581), April 1991.

108. J. D. Landes, *Extrapolation of the J-R Curve for Predicting Reactor Vessel Integrity*, USNRC Report NUREG/CR-5650 (ORNL/Sub/89-99732/1) (to be published).

109. This report.

1. INTRODUCTION

Traditionally, fracture mechanics has been focused on understanding fracture processes and providing fracture criteria for predicting the failure of structures with defects. In applications of linear-elastic fracture-mechanics (LEFM) methodology, mode I crack initiation is postulated to occur when the applied stress-intensity factor (K_I) exceeds a critical value (K_{Ic}) determined by material testing of small specimens, for example, compact (CT) specimens. However, in tests of large-scale single-edge-notched (SEN) tension wide-plate (WP) specimens[1] of A 533 grade B class 1 (A 533 B) steel, conducted by the Heavy-Section Steel Technology (HSST) Program at Oak Ridge National Laboratory (ORNL), cleavage-crack initiation occurred at K_I values well above those predicted by the small specimens. In fact, the K_I/K_{Ic} ratios ranged from 2.0 to 4.0. In Fig. 1, wide-plate data from the WP-1 series[1] are shown to be consistently in the upper scatter band of data from CT specimens. In response to this apparent failure of the fracture-mechanics approach, studies were initiated in the HSST Program to develop additional crack-tip stress field criteria incorporating effects of geometry, size, and thickness that would improve predictions of cleavage initiation in these reactor pressure vessel (RPV) steels.

ORNL-DWG 86-4886A ETD

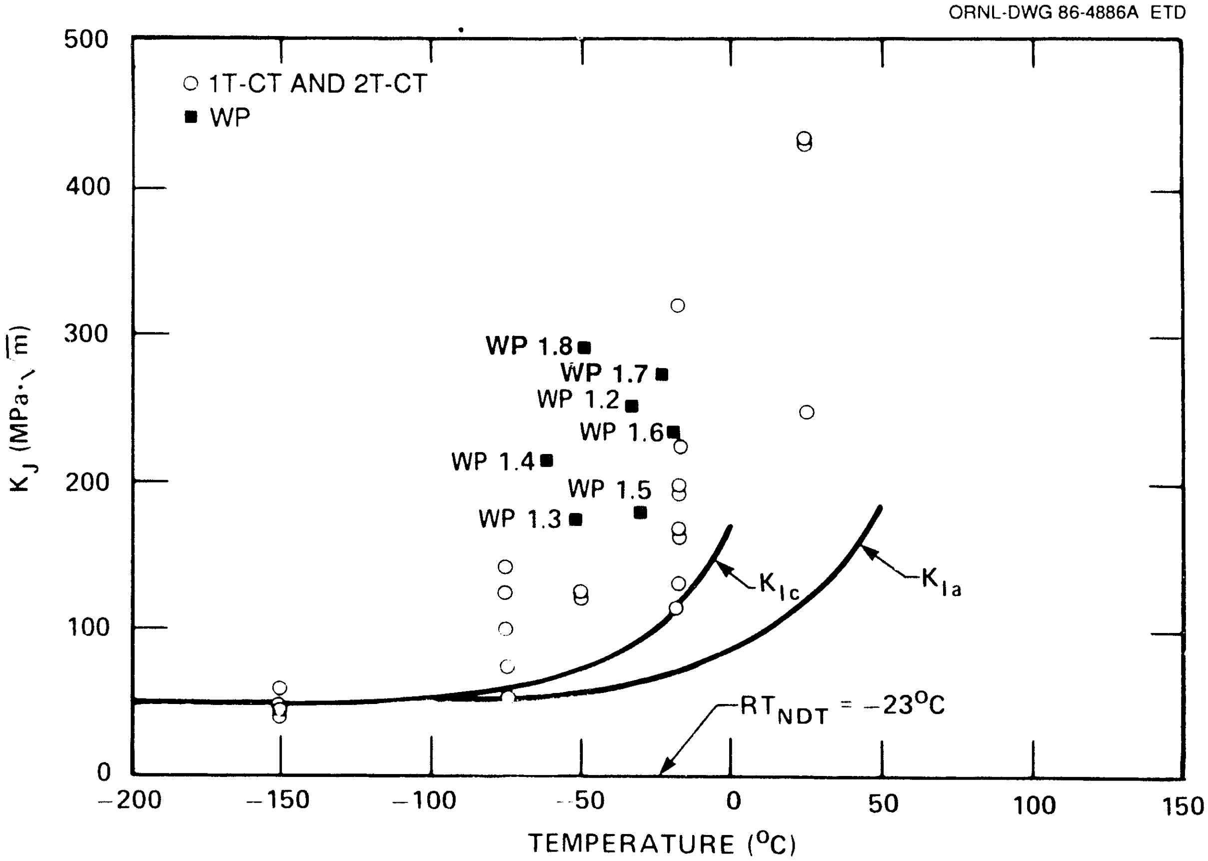

Fig. 1. Cleavage initiation values vs temperatures for small- and large-specimen tests of A 533 grade B class 1 steel.

The work centers around multidimensional analyses of the crack-tip stress fields in small-scale CT and large-scale WP geometries, modeling specimens previously tested under the HSST Program. All fracture data used in the study were measured on specimens taken from a single plate of A 533 B steel that had been extensively characterized for mechanical and fracture properties. Local crack-tip fields were generated from elastic-plastic analyses of two- and three-dimensional (2-D and 3-D) finite-element models of these test specimens. The crack-tip fields from these specimen analyses were used to evaluate correlation parameters that may be used to augment the K_I parameter for predicting cleavage initiation. The correlation parameters examined in this study are hydrostatic constraint and magnitude of maximum principal stress evaluated volumetrically ahead of the crack tip.

Section 2 summarizes material characterization of the A 533 B steel source plate for the test specimens, and Sect. 3 describes the CT and WP testing programs that provided the cleavage fracture-toughness data for the present study. In Sect. 4, a description is given of the cleavage initiation correlation parameters evaluated in this study. This is followed in Sect. 5 by a detailed description of the posttest fracture analyses of the CT and WP specimens, as well as an assessment of the fracture-toughness correlation parameters derived from the local crack-tip fields of the specimens. Finally, in Sect. 6, recommendations are made concerning the predictive capabilities of a dual-parameter model for cleavage initiation toughness in RPV steels.

2. MATERIAL CHARACTERIZATION

The first series of WP crack-arrest test specimens[1] and the CT test specimens used in this study were taken from HSST plate 13A, which is of A 533 B steel. Properties of the plate material included Young's modulus, E = 206.9 GPa; Poisson's ratio, $\nu = 0.3$; thermal expansion coefficient, $\alpha = 11 \times 10^{-6}$/°C; and density, $\rho = 7850$ kg/m^3. The average room-temperature tensile properties (longitudinal orientation) are as follows: ultimate tensile strength, 597 MPa; yield strength, 445 MPa; total elongation, 24%; and reduction in area, 69%.

Variations of longitudinal tensile properties with temperature for the plate center are shown in Fig. 2. Multilinear representations of the stress-strain curves for the material, with temperature as a parameter, are shown in Fig. 3. The temperature-dependent yield stress for the multilinear representations in this figure is given by the function

$$\sigma_y = 374.866 + 59.894e^{-0.0079328T} , \tag{1}$$

where σ_y and T are in megapascals and degrees Celsius, respectively. The stress-plastic-strain modulus H′(T) as a function of temperature is presented in Table 1.

Figure 4 shows that the Charpy V-notch (CVN) properties in the longitudinal orientation also did not vary appreciably through the plate thickness. The LT orientation has the specimen

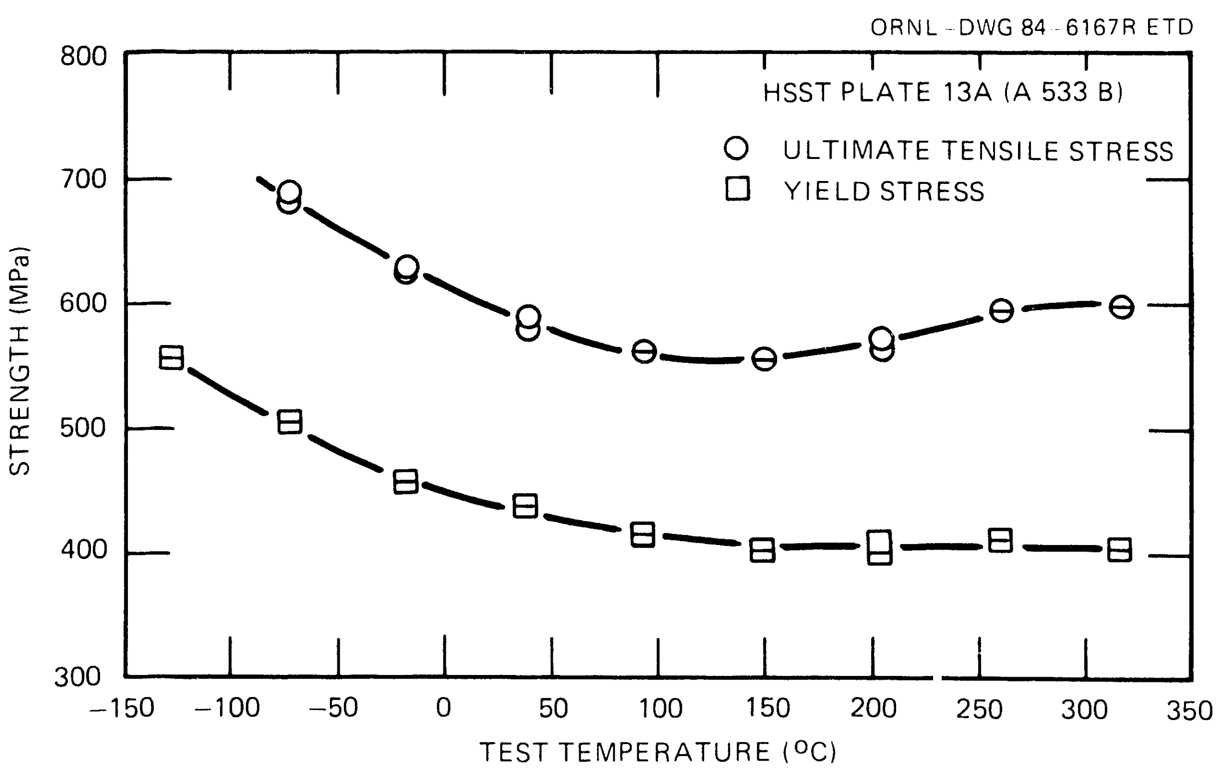

Fig. 2. Effect of temperature on longitudinal tensile properties for HSST plate 13A, A 533 grade B class 1 steel (specimens from center half of 18.7-cm-thick plate).

ORNL-DWG 85-4319R ETD

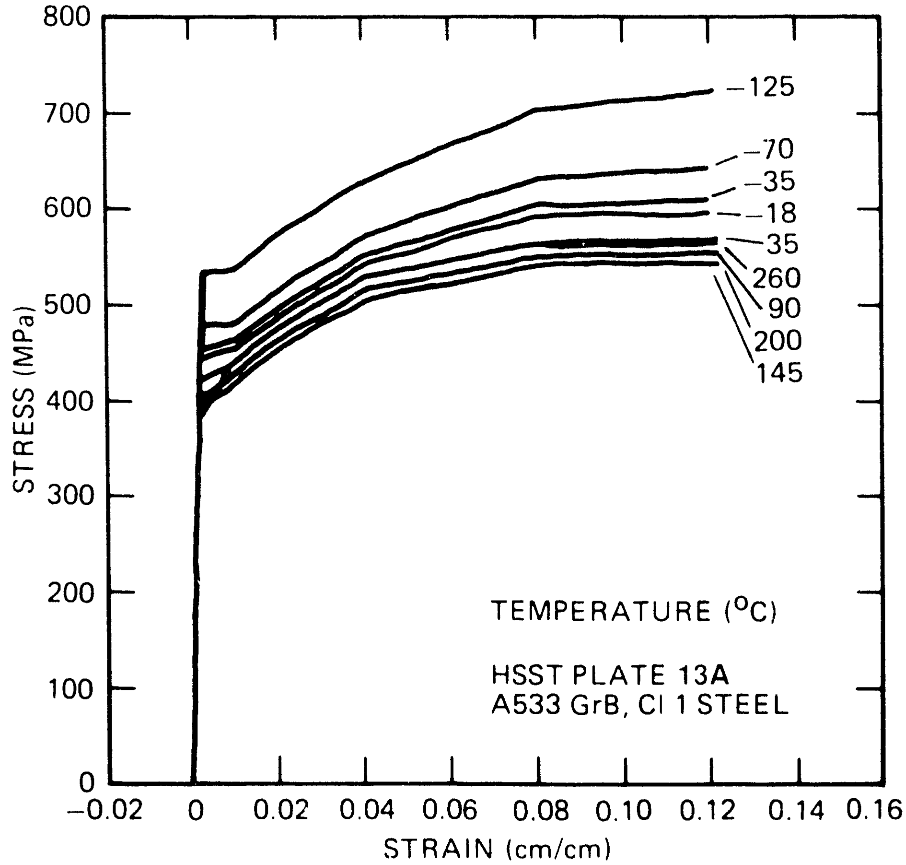

Fig. 3. Multilinear representations of uniaxial stress-strain behavior of HSST plate 13A of A 533 grade B class 1 steel.

Table 1. Stress-plastic-strain modulus H′ for HSST wide-plate material (HSST plate 13A of A 533 grade B class 1 steel)

Plastic strain interval (%)	Temperature interval (°C)	$H' = \Delta\sigma/\Delta\varepsilon^P$ (MPa/%)
<1	$-125.00 < T < -72.78$	0.345
	$-72.78 \le T < 37.78$	16.044 + 0.214 T
	$37.78 \le T < 148.89$	21.787 + 0.062 T
	$148.89 \le T < 260.00$	−24.407 + 0.372 T
1–2	$-125.00 < T < 260.00$	37.23
2–4	$-125.00 < T < 260.00$	26.579 − 0.00776 T
4–8	$-125.00 < T < 37.78$	11.228 − 0.0599 T
	$37.78 \le T < 260.00$	8.96
8–12	$-125.00 < T < -17.78$	−0.0276 − 0.0403 T
	$-17.78 \le T < 260.00$	0.689

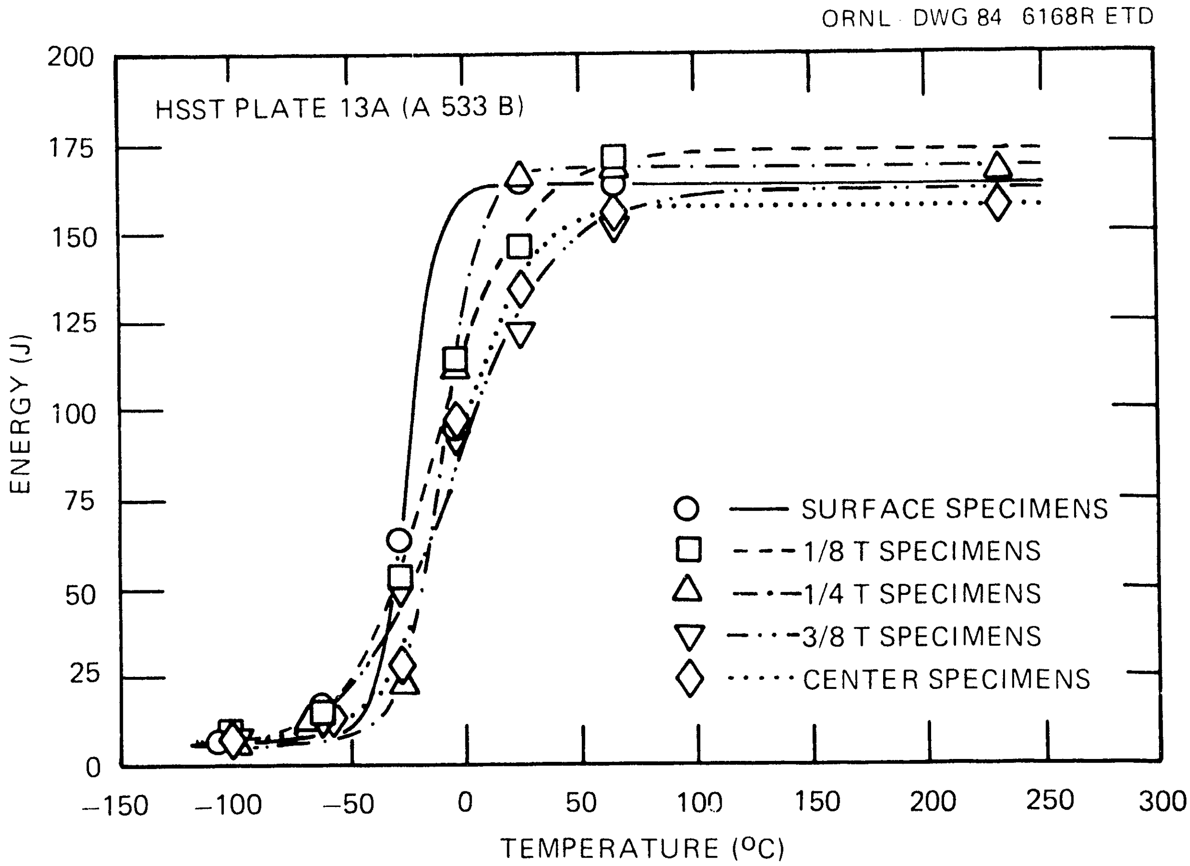

Fig. 4. CVN through-thickness results for LT specimens from HSST plate 13A, A 533 grade B class 1 steel in quenched and tempered condition.

parallel to the rolling direction and the notch (crack propagation) transverse to the rolling direction, similar to that for the WP crack-arrest specimens. For the center 100 mm of the plate, which was the portion used for the WP testing, the average 41-J transition temperature is –30°C, the 50% ductile transition temperature is 2°C, the upper-shelf energy is 160 J, the onset of upper-shelf energy is at 55°C, and 35 mils lateral expansion is obtained at –13°. The RT_{NDT} [American Society of Mechanical Engineers (ASME) reference nil-ductility temperature] was determined to be –23°C, as measured by drop-weight and Charpy testing in the LT orientation.

The fracture-toughness properties of HSST Plate 13A were determined at ORNL using 25.4- and 50.8-mm CT specimens (1T-CT and 2T-CT, respectively) modified for load-line displacement measurement.[1] The single-specimen unloading compliance technique of ASTM E1152 was used to measure crack growth during testing. The specimens were loaded under load-line displacement control at a rate of 0.2 mm/min. When applicable, K_{Ic} values were determined according to ASTM E399. Otherwise, the modified Ernst J-integral was used to infer K_{Ic} values from the relation

$$K_{Jc} = \sqrt{EJ_c} \, , \tag{2}$$

where

$$E(\mathrm{GPa}) = 207.2 - 0.057\ T\ (^\circ\mathrm{C})\ . \tag{3}$$

A plasticity correction ("beta-correction") was determined from the K_J value at cleavage using the Merkle method.[2] A summary of the fracture-mechanics tests is provided in Table 2. The material tearing resistance is represented by a power law curve having the equation

$$J_R = c(\Delta a)^m\ , \tag{4}$$

where c = 0.3539, m = 0.4708, and the units of J_R and Δa are megajoules per square meter and millimeters, respectively.

Fracture-toughness relations for crack initiation and arrest have been developed on the basis of small-specimen data and are given as follows:

$$K_{Ic} = 51.276 + 51.897e^{0.036(T - RT_{NDT})} \tag{5}$$

$$K_{Ia} = 49.957 + 16.878e^{0.029(T - RT_{NDT})}\ . \tag{6}$$

Units for K and T are megapascals times square root meters and degrees Celsius, respectively.

Table 2. Fracture-toughness results for wide-plate specimen (WP-1) material (HSST plate 13A, A 533 B steel)

Specimen	Test temperature (°C)	Thickness (mm)	a/w_i	Ductile Δa (mm)	J_{max} (kJ/m^2)	J_{cleave} (kJ/m^2)	K_{Jc} ($MPa\cdot\sqrt{m}$)	$K_{Jcleave}$ ($MPa\cdot\sqrt{m}$)	Beta-corrected $K_{Jcleave}$ ($MPa\cdot\sqrt{m}$)
K33A	−150	50.8	0.554	<0.020	9.2	9.2	44.6	44.6	44.2
K33B	−150	50.8	0.555	<0.200	15.8	15.8	58.4	58.4	57.0
K34A	−75	50.8	0.556	0.071	97.5	97.5	143.6	143.6	102.7
K34B	−18	50.8	0.562	0.366	242.7	242.7	203.8[a]	224.8	119.9
K35A	−150	50.8	0.555	<0.020	10.2	10.1	46.7	46.7	46.2
K35B	−150	50.8	0.543	<0.020	7.5	7.5	40.2	40.2	40.0
K41B	−18	50.8	0.563	0.221	195.9	195.9	202.0	202.0	114.7
K42B	−75	50.8	0.563	<0.020	49.1	49.1	101.9	101.9	84.8
K41A	−75	50.8	0.557	<0.020	64.3	64.3	116.6	116.6	92.1
K42A	−75	50.8	0.554	<0.020	63.8	63.8	116.2	116.2	91.9
K51C	−75	25.4	0.554	<0.020	14.4	14.4	55.2	55.2	50.7
K52B	−75	25.4	0.576	<0.020	26.3	26.3	74.6	74.6	62.5
K53E	−18	25.4	0.562	0.196	177.6	177.6	192.3	192.3	91.5
K53F	−18	25.4	0.572	0.064	64.5	64.5	115.9	115.9	74.0
K54A	−75	25.4	0.573	<0.020	74.1	74.1	125.2	125.2	82.6
K54F	−18	25.4	0.568	1.122	124.4	124.4	160.9	160.9	85.2

[a] J_{Ic} used to calculate K_{Jc}; otherwise J_{max} load used.

3. WIDE-PLATE TESTING PROGRAM AND TEST DATA

The primary objective of the wide-plate crack-arrest studies[1,3–7] was to generate data and associated analysis methods for understanding the crack-arrest behavior of prototypical RPV steels at temperatures near and above the onset of the Charpy upper-shelf region. Program goals included (1) extending the existing K_{Ia} data bases to values above those associated with the upper limit in the American Society of Mechanical Engineers Boiler and Pressure Vessel Code (ASME B&PVC); (2) clearly establishing that crack arrest occurs prior to fracture-mode conversion; and (3) validating the predictability of crack arrest, stable tearing, and/or unstable tearing sequences for RPV materials. Sixteen WP crack-arrest tests were completed, ten utilizing specimens fabricated from A 533 B material and six fabricated from a low-upper-shelf base material.

The 1- × 1- × 0.1-m (WP-1.2 through WP-1.6) or 1- × 1- × 0.15-m (WP-1.7 and WP-1.8) WP specimens were machined and precracked by ORNL. The precracking was done by hydrogen charging an electron-beam (EB) weld located at the base of a premachined notch in the plate. The initial total crack length, notch depth plus EB weld, for each specimen was nominally 0.2 m (a/W ~ 0.2). Each face of a specimen was grooved to a depth equal to 12.5% of the plate thickness. Starting with the third specimen in test series WP-1 (WP-1.3), the crack front of each specimen was machined into a truncated chevron configuration to reduce the tensile load required to achieve crack initiation. Upon completion of the machining operations, each specimen was shipped to the National Institute of Standards and Technology (NIST) in Gaithersburg, Maryland, where it was welded to pull plates nominally having the same cross-section geometry as the specimen to produce the test article shown schematically in Fig. 5.

To obtain pertinent data during a test, each WP specimen was instrumented with three primary types of devices: (1) thermocouples; (2) strain gages; and (3) crack-opening displacement (COD) gages. Also, an acoustic emission transducer was located on the lower pull tab of each specimen. After being instrumented, the specimen was placed into the 27-MN-capacity tensile testing machine, and electric-resistance strip heaters were attached to the back edge of the plate. A temperature gradient was imposed across the plate by spraying liquid nitrogen (LN_2) onto the notched edge while heating the other edge. Generally, the midplate (a/W = 0.5) temperature was selected to correspond to that of the onset of Charpy upper-shelf energy (USE) for the material tested, and the crack-tip temperature was varied to provide the desired initiation load. Upon obtaining the desired temperature gradient, tensile load was applied to the specimen at a rate which varied from 11 to 312 kN/s, depending on the test, until fracture occurred. Table 3 presents a summary of the conditions for testing of the A 533 B wide-plate materials. A detailed description of each of these tests is provided elsewhere.[1,3–7]

Initiation stress-intensity factors obtained from tests in the WP-1 series are compared in Table 4. In Fig. 1, the WP-1 initiation K_I values are compared with the CT-specimen data from Table 2.

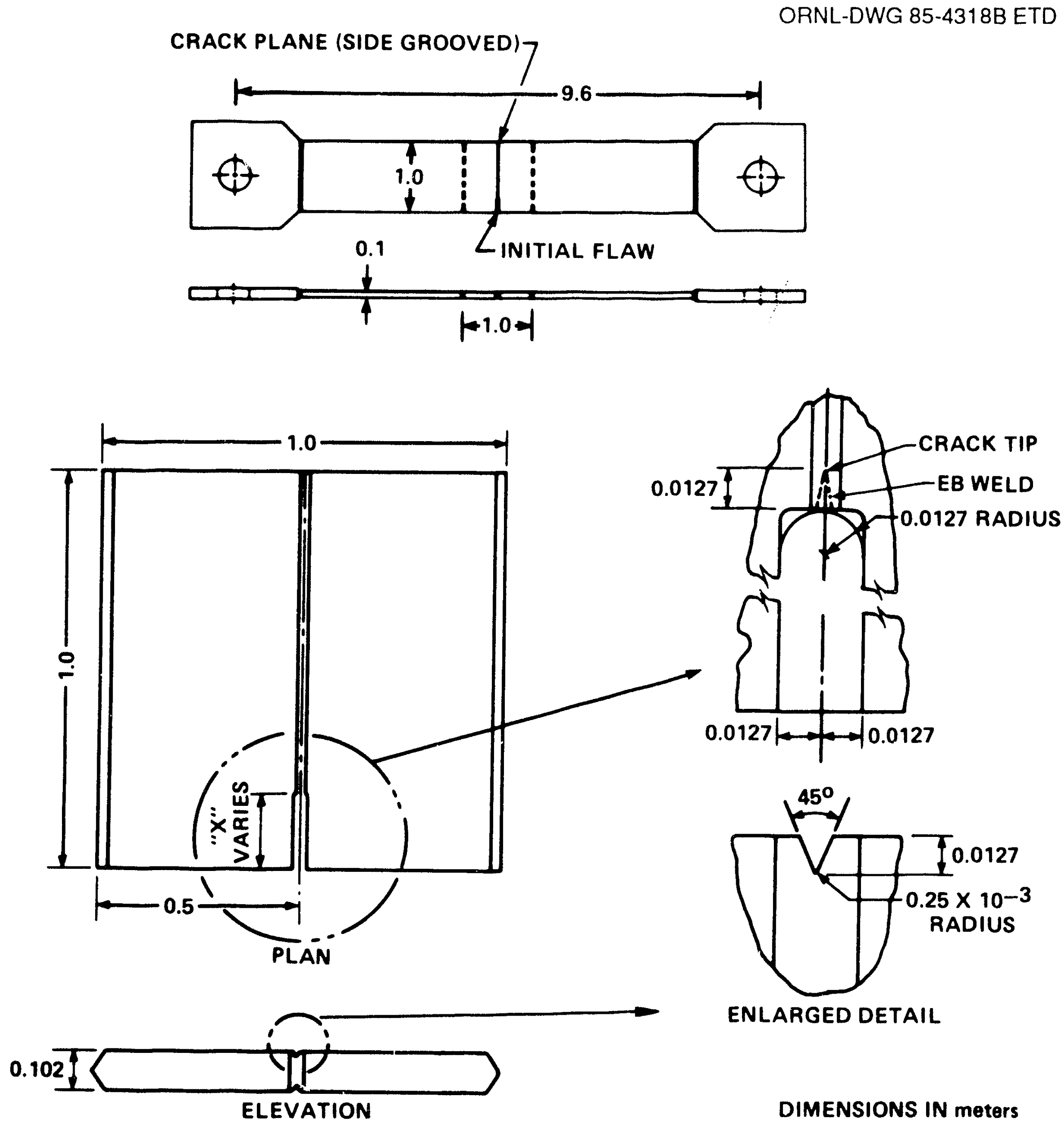

Fig. 5. Schematic of HSST wide-plate crack-arrest specimen.

Table 3. Summary of HSST wide-plate crack-arrest test conditions and results for A 533 grade B class 1 steel: WP-1 series

Test No.	Crack location (cm)	Crack temperature (°C)	Initiation load (MN)	Arrest location (cm)	Arrest temperature (°C)	Arrest $T - RT_{NDT}$ (°C)	Crack-arrest toughness[a] $(MPa \cdot \sqrt{m})$
WP-1.1[b]	20.0	–60	20.10	50.2	51	74	NA
WP-1.2A	20.0	–33	18.90	55.5	62	85	424
WP-1.2B	55.5	62	18.90	64.5	92	115	685
WP-1.3	20.0[c]	–51	11.25	48.5	54	77	235
WP-1.4A	20.7[c,d]	–63	7.95	44.1	29	52	NA
WP-1.4B	44.1	29	9.72	52.7	60	83	387
WP-1.5A	20.0[c]	–30	11.03	52.1	56	79	231
WP-1.5B	52.1	56	11.03	58.0	72	95	509
WP-1.6A	20.0[c]	–19	14.50	49.3	54	77	275
WP-1.6B	49.3	54	14.50	59.3	80	103	397
WP-1.7A	20.2[c]	–24	26.20	52.8	61	84	319
WP-1.7B	52.8	61	26.20	63.5	88	111	555
WP-1.8A	19.8[c]	–47	26.50	44.9	40	63	345
WP-1.8B	44.9	40	26.50	50.4	55	78	484
WP-1.8C	50.4	55	26.50	59.4	79	102	563

[a]Dynamic finite-element analyses.
[b]Specimen was warm prestressed by loading to 10 MN at 70°C. Specimen was also preloaded to 19 MN.
[c]Crack front was cut to truncated chevron configuration.
[d]Pillow jack was used to apply pressure load to specimen's machined notch.

Table 4. Initiation stress-intensity factor comparisons for the WP-1 series of wide-plate crack-arrest tests

Test designation	Crack-tip temperature (°C)	Calculated static K_I $(MPa \cdot \sqrt{m})$	Property correlation K_{Ic}[a] $(MPa \cdot \sqrt{m})$	K_I/K_{Ic}
WP-1.2	–33.0	251.5[b]	87.5	2.87
WP-1.3	–51.0	173.5[c]	70.1	2.48
WP-1.4	–62.0	213.0[c]	63.9	3.33
WP-1.5	–30.0	179.8[c]	91.6	1.96
WP-1.6	–19.0	233.8[c]	111.2	2.10
WP-1.7	–22.7	280.6[c]	103.7	2.71
WP-1.8	–47.2	290.0[c]	73.0	3.97

[a]Calculated from $K_{Ic} = 51.276 + 51.897e^{0.036\,(T - RT_{NDT})}$ using crack-tip temperature of initial flaw and material RT_{NDT}.
[b]Computed from 2-D static analysis.
[c]Computed from 3-D static analysis.

4. FRACTURE-TOUGHNESS CORRELATION PARAMETERS

The variability of cleavage fracture-toughness values for pressure vessel steels (as a function of temperature) is well-documented in the literature (see, for example, Refs. 8–14). As discussed by Merkle,[2] this variability can be traced to physical effects, such as difference in size and geometry of test specimens, and to the existence of scatter due to material variability. A large body of literature has developed which examines physical effects based on experimental methods or on micromechanical models,[9–11,15–17] while material variability has been modeled using statistical methods.[12–14] The emphasis in this study is on the resolution of physical effects through the use of correlation parameters based on local crack-tip stress fields. These parameters are described in the following sections.

4.1 HYDROSTATIC CONSTRAINT

The cleavage fracture model, described by Kanninen and Popelar,[18] is based on the conditions of small-scale yielding; that is, the size of the plastic zone ahead of the crack tip is small compared to the K-dominant region, and the crack-tip stresses and strains are uniquely characterized by K or J. However, with increasing plasticity, small-scale yielding conditions and K-dominance are eventually lost, and K-values at initiation become size dependent. Generally, the loss of K-dominance leads to a reduction in triaxiality, which can be quantified conveniently in terms of constraint factors. One type of constraint factor is the ratio of the hydrostatic stress to the Von Mises effective stress:

$$h = \sigma_H/\sigma_v \ , \tag{7}$$

with

$$\sigma_H = (\sigma_{XX} + \sigma_{YY} + \sigma_{ZZ})/3 \ , \tag{8}$$

and

$$\sigma_v = \left\{3\left[0.5\left(\sigma'^2_{XX} + \sigma'^2_{YY} + \sigma'^2_{ZZ}\right) + \sigma^2_{XY} + \sigma^2_{YZ} + \sigma^2_{XZ}\right]\right\}^{1/2} \ , \tag{9}$$

where σ_v is proportional to the square root of the second invariant of the deviatoric stress tensor. A function of this ratio has been used previously by Rice and Tracey[19] to predict macroscopic fracture toughness using microscopic void growth models. A higher value of the constraint factor h indicates a higher degree of triaxiality. When triaxiality is high, the plastic flow of the material decreases, thereby inhibiting the ability of the material to reduce local stress peaks. According to Merkle,[2] triaxiality is necessary to sustain cleavage-microcrack propagation in normal structural steels because the maximum principal tensile stress must be equal to or greater than the cleavage fracture stress when the maximum principal tensile strain reaches the cracking strain of the grain boundary carbide, which is about 2%.

The hydrostatic stress, and consequently the constraint factor h, in the plastic zone ahead of the crack tip depend on the transverse strain, that is, the strain parallel to the crack front. For through-cracked specimens such as CT and WP configurations, the transverse strain depends on the ratio of the plastic-zone size to the thickness. When the plastic zone becomes large compared to the plate thickness, yielding can take place freely in the thickness direction (condition of plane stress). As the transverse contraction strain increases, the maximum hydrostatic stress and the maximum principal tensile stress on the crack plane ahead of the crack tip decrease. Consequently, the load and the plastic-zone size at cleavage initiation are increased, with an apparent elevation in the fracture toughness of the material.

4.2 MAXIMUM PRINCIPAL STRESS

In an early study, Richie, Knott, and Rice[15] developed a relationship between tensile stress and cleavage fracture toughness in a mild steel under plane-strain conditions. In their study, unstable cleavage fracture is postulated to occur when the maximum principal stress exceeds a critical value of stress over a characteristic distance ahead of the crack tip, determined as twice the grain size of the material. The results in Ref. 15 are based on elastic-plastic solutions for the stress distribution ahead of a sharp crack. The use of a sharp-crack model necessitated that the critical stress be achieved over some microstructurally significant distance ahead of the crack tip to avoid predictions of fracture at vanishingly small loads due to the stress singularity.

Merkle[2] asserts that a description of the crack-tip stress and strain fields required to model the onset of cleavage fracture can be attained only by considering the blunting of the crack tip. Crack-tip blunting leads to a finite crack-tip root radius, with zero stress normal to the blunted crack surface. Thus, the point of greatest hydrostatic stress occurs at a small distance ahead of the notch tip, while the greatest strain occurs at the notch tip. Finite deformation analyses performed by McMeeking[20] and McMeeking and Parks[21] indicate that the point of maximum stress is approximately $3\delta_t$ ahead of the crack tip, where δ_t is the crack-tip opening displacement. Merkle[2] points out that the blunted crack-tip model eliminates the necessity of exceeding the critical stress over a characteristic distance to cope with a nonexistent stress singularity, such as the criterion of Ref. 15. However, Dodds and Anderson[17] point out that relaxation of stresses near the free surface of the blunted tip implies that the fracture process zone lies beyond the finitely deforming zone adjacent to the tip. They argue that, because differences in stresses from small-strain and finite deformation analyses of the small-scale yielding model become insignificant beyond $3\delta_t$ from the crack tip, small-strain solutions are adequate to assess crack-tip fields for the stress-controlled cleavage process.

In recent studies, Anderson and Dodds[16] constructed a correlation procedure to remove the geometry dependence of cleavage fracture-toughness values for single-edge-notched bend (SENB) specimens of A36 steel for a range of crack depths. This procedure utilizes a local stress-based criterion for cleavage fracture and detailed plane-strain finite-element analysis. From Ref. 16, dimensional analysis for small-scale yielding implies that the principal stress ahead of the crack tip can be written as

$$\frac{\sigma_1}{\sigma_o} = f\left(\frac{J^2}{\sigma_o^2 A}\right) , \tag{10}$$

where σ_o is the 0.2% offset yield strength, σ_1 is the maximum principal stress at a point, and A is the area enclosed by the contour on which σ_1 is a constant. The strategy employed in Ref. 16 utilizes a fracture criterion dependent upon achieving a critical volume $V(\sigma_1)$ within which the principal stress is greater than σ_1. For a specimen subjected to plane-strain conditions, the volume is equal to the specimen thickness B times the area within the σ_1 contour on the midplane ($V = BA$). Thus Eq. (10) is the appropriate normalization for small-scale yielding solutions when using the latter fracture criterion based on volume or area.

In the following, correlations are developed between local crack-tip fields in CT and WP specimens utilizing parameters discussed in this section. Specifically, these include a comparison of the hydrostatic constraint factor, h, for the various loading conditions and a volumetric (or area) maximum principal stress criterion, based on volume $V(\sigma_1)$ [or area $A(\sigma_1)$] and a critical stress σ_1. These criteria are applied to analysis results from both 2-D and 3-D finite-element models of CT and WP specimen geometries that were tested in the HSST Program.

5. POSTTEST ANALYSES AND EVALUATION OF LOCAL CRACK-TIP FIELDS

Two-dimensional plane-stress and plane-strain and fully 3-D finite-element models were employed to generate the local crack-tip fields for the CT and WP specimens. The numerical analysis techniques utilized both small- and large-strain formulations and the constitutive model representation for A 533 B steel described in Sect. 2. In the following, detailed descriptions of these models are given, as well as the loading conditions for each analysis performed. Interpretations of the results are discussed in terms of the fracture correlation parameters of Sect. 4, which are evaluated from the local crack-tip fields of the finite-element analyses.

5.1 FINITE-ELEMENT MODELS

The 2-D finite-element model of the CT configuration used in the nonlinear elastic-plastic analyses consists of 1852 nodes and 580 eight-noded isoparametric elements, as shown in Fig. 6. Collapsed-prism elements surround the crack tip to allow for blunting and for a 1/r singularity in the strains at the crack front. The radial dimension of the collapsed-prism elements at the crack tip is r = 0.22 mm (r/w = 0.0043) for the 1T-CT specimen and r = 0.44 mm (r/w = 0.0043) for the 2T-CT specimen.

The 3-D finite-element models of the CT specimens were generated by projecting the planform of a 2-D mesh for each specimen through the thickness, using four elements in the thickness direction. The 3-D finite-element model of the 1T- and 2T-CT specimens consists of 6344 nodes, 1088 20-noded isoparametric brick elements, and 112 collapsed-prism elements at the crack front for a 1/r singularity. One quarter of the specimen is modeled because of symmetry. The model for the 2T-CT specimen is shown in Fig. 7.

The 2-D finite-element model for the WP specimens consists of 1164 nodes and 348 eight-noded isoparametric elements. The collapsed-prism elements at the crack tip have radial dimensions of r = 0.375 mm (r/w = 0.000375). The 3-D finite-element model of the WP specimens consists of 7542 nodes, 1297 20-noded isoparametric brick elements, and 112 collapsed prism elements at the crack front. The WP model is shown in Fig. 8; a detailed plot of the crack-tip region is given in Fig. 9. For the 3-D model, the radial dimension of the collapsed-prism crack-tip elements is r = 0.75 mm (r/w = 0.00075), which is twice that for the 2-D model.

5.2 FINITE-ELEMENT RESULTS AND EVALUATIONS OF CRACK-TIP FIELD PARAMETERS

Two-dimensional plane-stress and plane-strain analyses were performed using the 2T-CT specimen model and the multilinear true stress-strain curves from Fig. 3, assuming uniform temperatures of −150, −75, and −18°C. A material-nonlinear-only (MNLO) formulation (small-strain theory) was used in these analyses. The load was applied incrementally in the form of a cosine stress distribution function to the load pin hole up to the load where crack initiation took place for each 2T-CT test. By comparing the plane-strain and plane-stress solutions for load vs displacement, it was observed that the experimental data plot close to the calculated plane-strain curve (see Fig. 10).

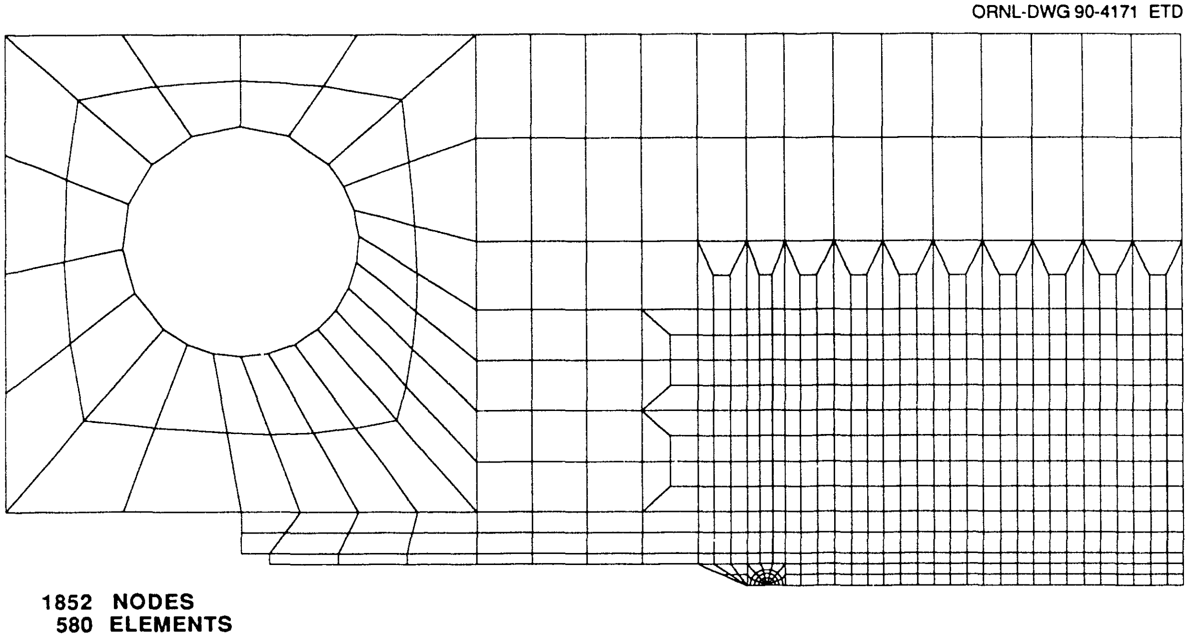

Fig. 6. Two-dimensional finite-element model for the 2T-CT specimen.

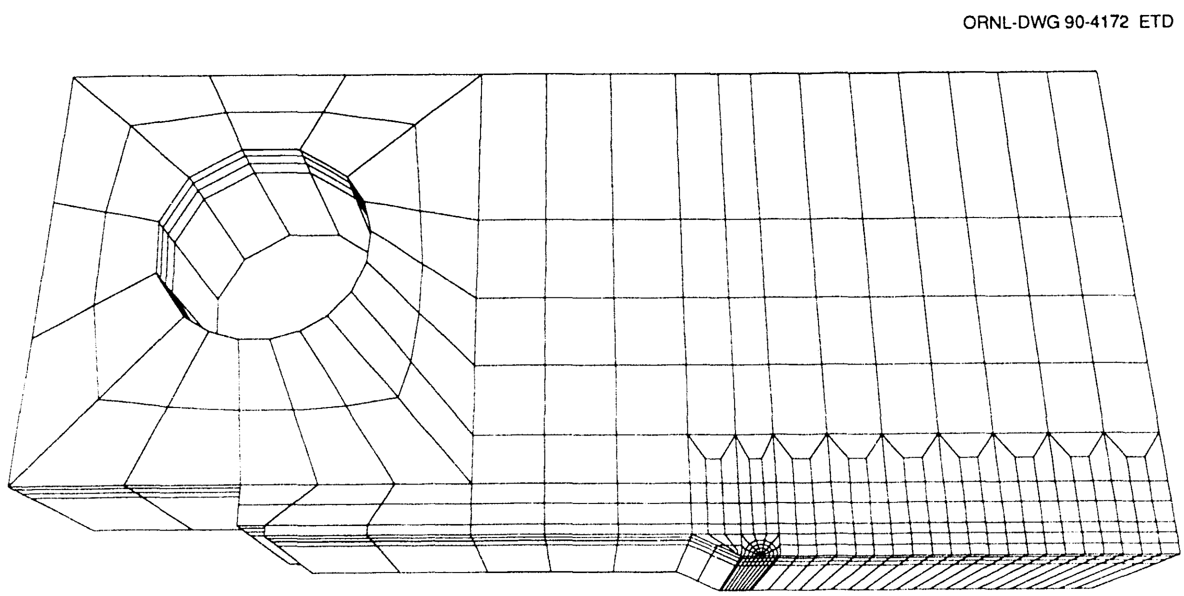

Fig. 7. Three-dimensional finite-element model for the 2T-CT specimen.

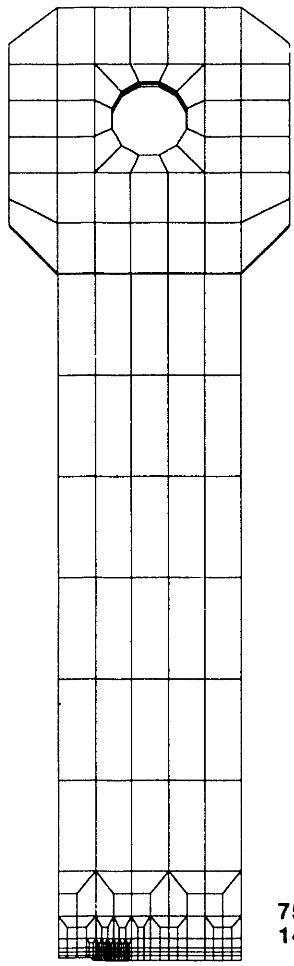

Fig. 8. Three-dimensional finite-element model for the WP specimen.

For the 3-D models of the CT specimens, elastic-plastic static analyses were performed at temperatures of −150°C for the 2T-CT specimen and −75°C for the 1T- and 2T-CT specimens. An MNLO formulation with a multilinear true stress-strain curve was used for the 1T-CT specimen analysis. Since there had been some question concerning whether to use small-strain or large-strain theory for these analyses, two analyses were performed for the 2T-CT specimens at −75°C, utilizing MNLO and updated Lagrangian (UL) formulations (large-strain theory) with a bilinear (BL) true stress-strain curve. Figure 11 shows the variation of the constraint factor, h, given by Eqs. (7)–(9), with the distance from the crack tip at −75°C. For the MNLO formulation, all the 3-D analyses fall on the 2-D plane-strain curve, and the value for h increases steeply toward the crack tip. For the UL analysis, the value of h begins to decrease after a maximum at about 0.4 mm (~4 δ_t) from the crack tip. Similar trends were reported in Ref. 22.

Elastic-plastic plane-strain analyses were performed using the 2-D WP finite-element model and an MNLO formulation. Because these analyses were concerned with crack initiation, the specimen was assumed to be in an isothermal condition at the crack-tip temperature

ORNL-DWG 90-4174 ETD

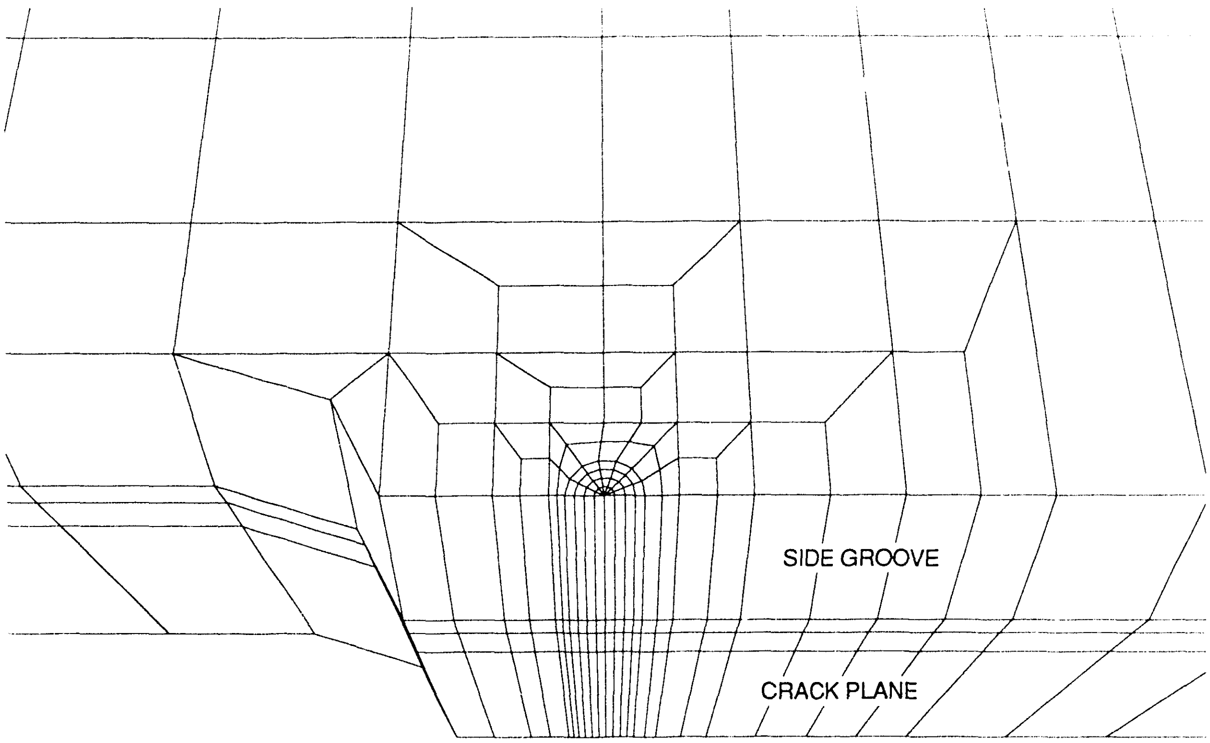

Fig. 9. Crack-tip region of the 3-D finite-element model for the WP specimen.

measured in each WP test. A multilinear true stress-strain curve corresponding to this temperature was selected from Fig. 3 for each analysis. The calculated J values were elevated by the ratio of crack front-to-wide plate thicknesses to approximate in a 2-D model the conditions produced by side grooves and the chevron.

A thermo-elastic-plastic analysis of the 3-D WP model was carried out using an MNLO formulation and bilinear true stress-strain curves constructed from the multilinear curves of Fig. 3. Boundary conditions prescribed for the model also included the thermal gradient across the plate. In Fig. 12, the lower values of h for the WP analysis imply less constraint for the WP specimen than for the CT specimen. However, these values are still considered to be in the plane-strain range. When h is plotted through the thickness for both specimens (Fig. 13), the values at comparable r's would be slightly lower for the WP specimen than the CT specimen if the side-grooved region of the WP specimen is excluded. The side-groove of the WP specimen gives rise to stress peaks since it was modeled without a finite root radius. In the CT specimen, h is a maximum at center plane and decreases to the 2-D plane-stress value at the free surface. When the through-thickness average value, h_m, is plotted vs the stress-intensity factor (Fig. 14), constraint is higher for the WP specimen until $K \approx 25$ MPa $\cdot \sqrt{m}$. These results are similar to those observed in Ref. 22 for the CT specimens.

The fracture model based on maximum principal stress theory described in the previous section was applied to the analyses of the CT and WP specimens. A criterion for plane-strain fracture is based upon achieving a critical area, $A_{CR}(\sigma_1)$, within which the maximum principal

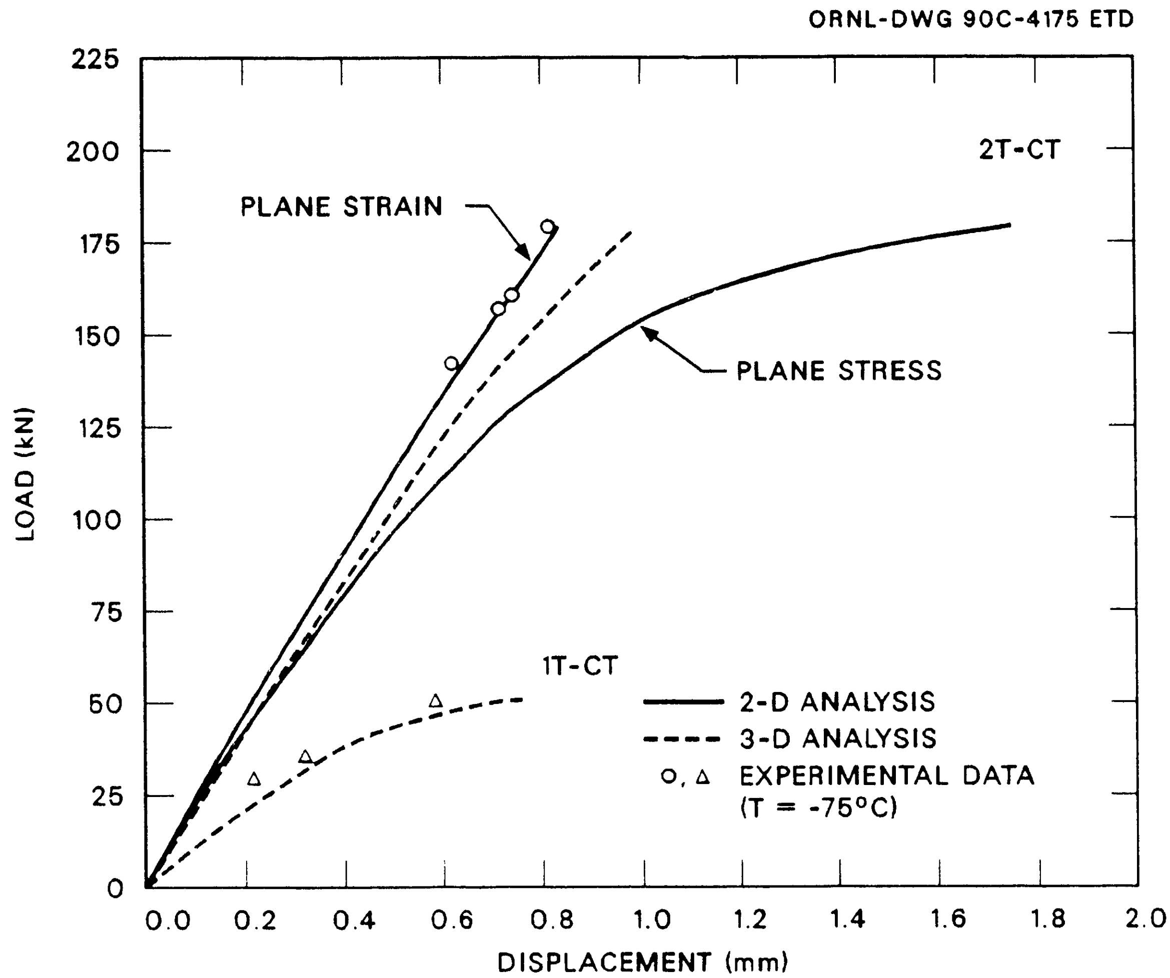

Fig. 10. Results of elastic-plastic analyses for the CT specimens at –75°C showing load vs crack-mouth opening displacement.

stress is greater than a chosen stress, σ_1. This criterion was applied to the analyses of the CT and WP specimens, and a portion of the results is summarized in Table 5. A maximum principal stress of σ_{p1} = 1400 MPa was used to generate the contour areas in Table 5. This critical stress is based on the average maximum principal stress calculated for the 2-D and 3-D analyses of the CT specimens. Also, Hahn, Gilbert, and Reid[23] estimated that the cleavage-microcrack propagation stress for individual grains of ferrite is 1380 MPa. In Table 5, the area within the stress contour σ_{p1} = 1400 MPa is tabulated as a function of load for the 2-D and 3-D finite-element solutions. When these areas are normalized with respect to the factor $(\sigma_o/J)^2$, the normalized values vary slightly for the 2T-CT specimen over the range of loading. By contrast, the normalized results for the WP specimens decrease significantly with increasing load after an initial increase, indicating loss of constraint with respect to small-scale yielding.

In the 2-D analyses of the CT specimens, the area corresponding to the smallest initiation load (0.144 MN) at –75°C is given by A_{CR} = 0.1316 mm^2. Comparing this with the area from the 2-D WP analyses, the same critical area is achieved at an applied load of approximately 15.7

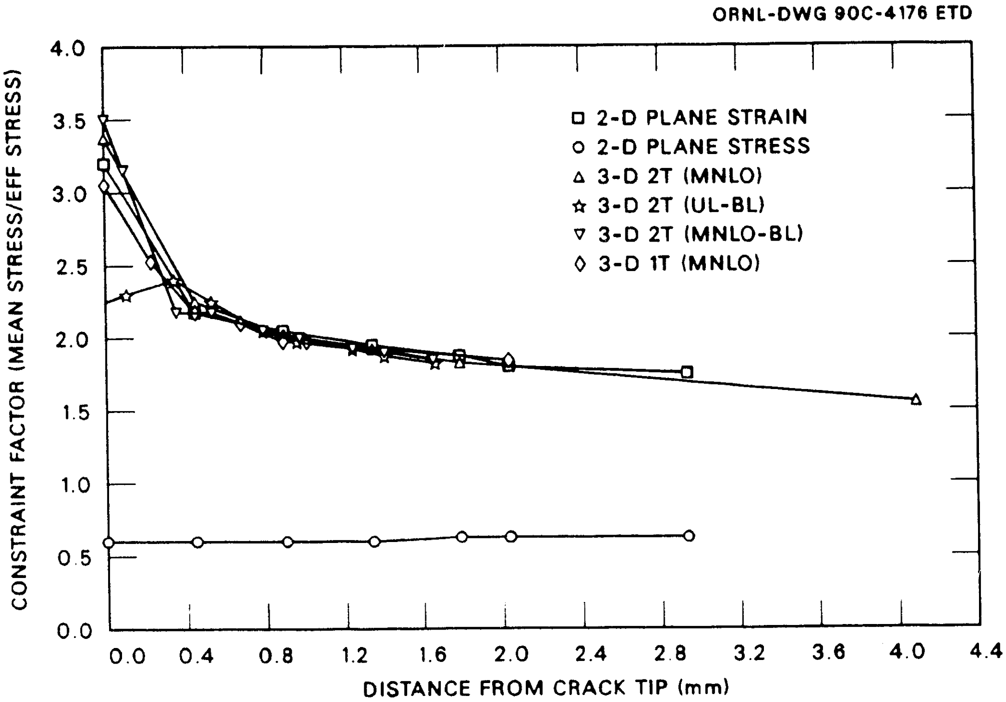

Fig. 11. Constraint vs distance from the crack tip from elastic-plastic analyses for the 1T- and 2T-CT specimens at –75°C.

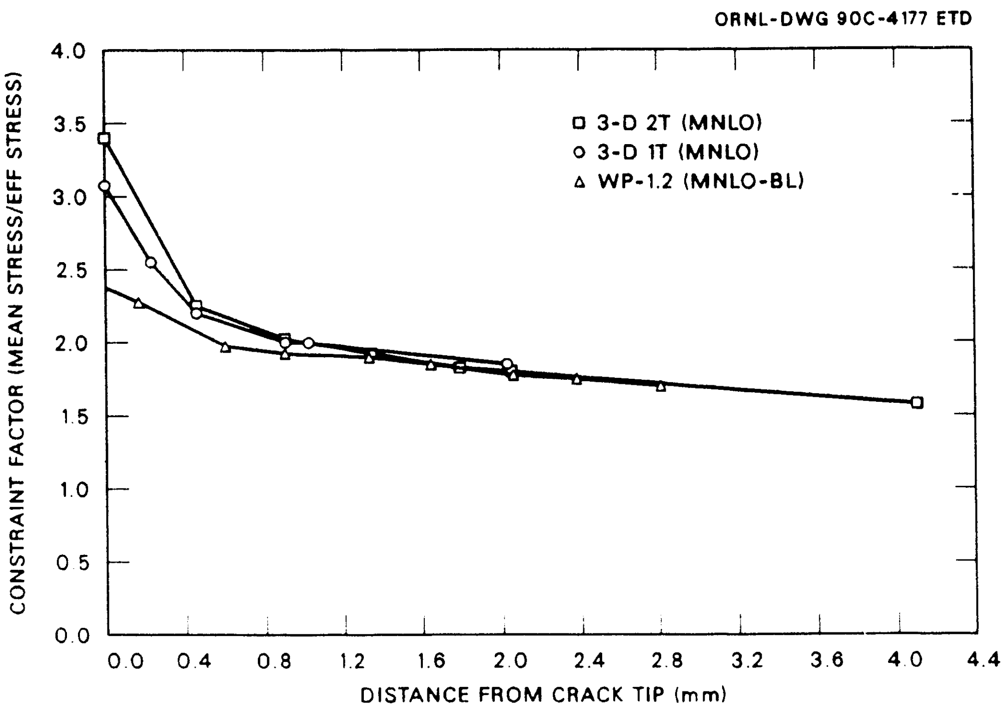

Fig. 12. Constraint vs distance from the crack tip from 3-D elastic-plastic analyses for the CT specimens at –75°C and the WP specimen at –33°C.

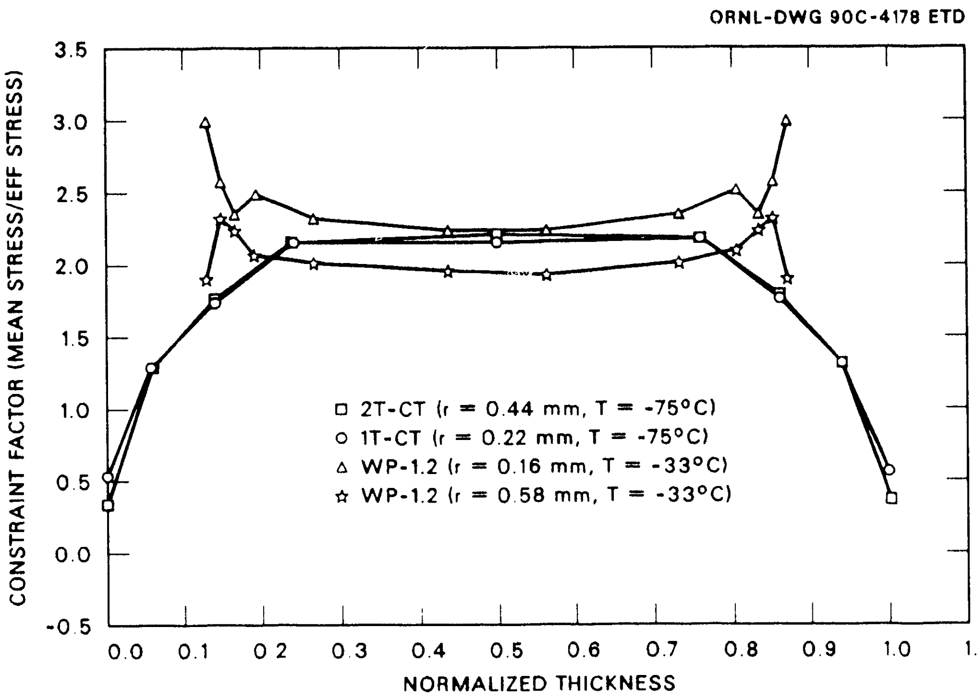

Fig. 13. Comparison of the through-thickness constraint for the CT and WP specimens from 3-D elastic-plastic analyses.

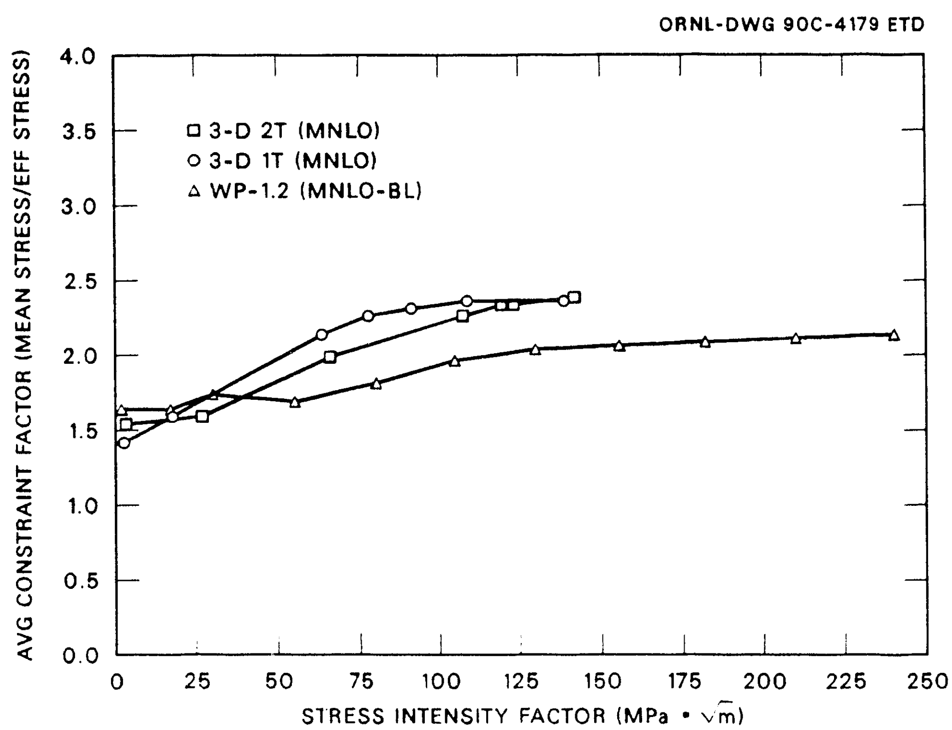

Fig. 14. Comparison of the through-thickness average constraint for increasing load for the CT specimens at –75°C and the WP specimen at –33°C from 3-D elastic-plastic analyses.

Table 5. Cumulative area within the maximum principal stress contour σ_{p1} = 1400 MPa for CT and wide-plate specimens

Specimen	Measured load (MN)	FEM calculated values			Remarks
		J (MJ/m^2)	Area (mm^2)	Normalized area $A^*(\sigma_0/J)^2$	
K42B	0.144	0.0480	0.1316	13.4	2T-CT[a]
K42A	0.158	0.0586	0.2166	14.8	
K41A	0.162	0.0615	0.2278	14.0	
K34A	0.180	0.0775	0.3572	14.0	
K41B	0.203	0.1075	0.2774	4.4	2T-CT[b]
K34B	0.207	0.1149	0.3002	4.4	2T-CT[b]
K51C	0.029	0.0173	0.0120	9.4	1T-CT[c]
Calculation only	0.031	0.0199	0.0120	7.0	
K52B	0.035	0.0262	0.0326	11.2	
K54A	0.050	0.0845	0.2544	8.4	
WP-1.3[d]	7.63	0.0476	0.0328	3.2	
	8.44	0.0583	0.0328	2.6	
	8.84	0.0640	0.1186	6.2	
	9.64	0.0764	0.1268	4.6	
	11.25	0.1044	0.1428	2.8	Fracture
WP-1.6[e]	7.46	0.0455	0.0090	0.8	
	8.29	0.0563	0.0202	1.2	
	8.70	0.0621	0.0338	1.8	
	9.53	0.0748	0.0338	1.2	
	14.50	0.1754	0.2538	1.6	Fracture
WP-1.2[f]	8.81	0.0512	0.0202	1.6	
	9.48	0.0595	0.0212	1.2	
	10.16	0.0685	0.0338	1.4	
	10.84	0.0780	0.0506	1.8	
	18.90	0.2440	0.2452	0.8	Fracture
WP-1.2[g]	5.34	0.0203	0.0974	48.4	
	11.49	0.0895	0.3952	10.2	
	18.90	0.2545	0.8802	2.8	Fracture

[a]2-D elastic-plastic static analysis at T = –75°C.
[b]2-D elastic-plastic static analysis at T = –18°C.
[c]3-D elastic-plastic static analysis at T = –75°C.
[d]2-D elastic-plastic static analysis at T = –51°C.
[e]2-D elastic-plastic static analysis at T = –19°C.
[f]2-D elastic-plastic static analysis at T = –33°C.
[g]3-D thermo-elastic-plastic static analysis with thermal gradient at T_{CT} = –33°C.

MN for WP-1.2, 10.06 MN for WP-1.3, and 10.83 MN for WP-1.6; the critical areas corresponding to the initiation loads are 0.2452, 0.1428, and 0.2538 mm^2, respectively. In Fig. 15, the applied J values calculated from the 2-D analyses for the 2T-CT and WP specimens are plotted vs the area within the critical stress contour, σ_{p1} = 1400 MPa, at each load step. For given values of A_{CR} and temperature, T, values of the J-integral for the WP specimen lie above those for the CT specimen, reflecting the differences in crack-tip constraint in these two geometries. Using the critical areas at initiation for the 2T-CT specimen at –75 and –18°C, a prediction can be made for J at initiation of the WP specimens. From the CT specimen results, the predicted A_{CR} values at initiation, at –75 and –18°C, are 0.234 and 0.288 mm^2, respectively. This implies that the J value at initiation for the WP specimen with a crack-tip temperature of –33°C should lie in the interval (0.233, 0.255) MJ/m^2. The calculated J value at initiation for WP-1.2 was 0.244 MJ/m^2.

A simple relation was developed for A_{CR} to account for the elevation of the stresses in front of a crack tip due to the presence of a chevron in WP-1.3 and WP-1.6. Two 3-D elastic analyses were performed with a chevroned and a nonchevroned wide plate to compare differences in the stresses at the crack plane. The wide plate was side-grooved in both analyses. While the stress ratio is variable, a mean value of 1.07 was used to increase the stress

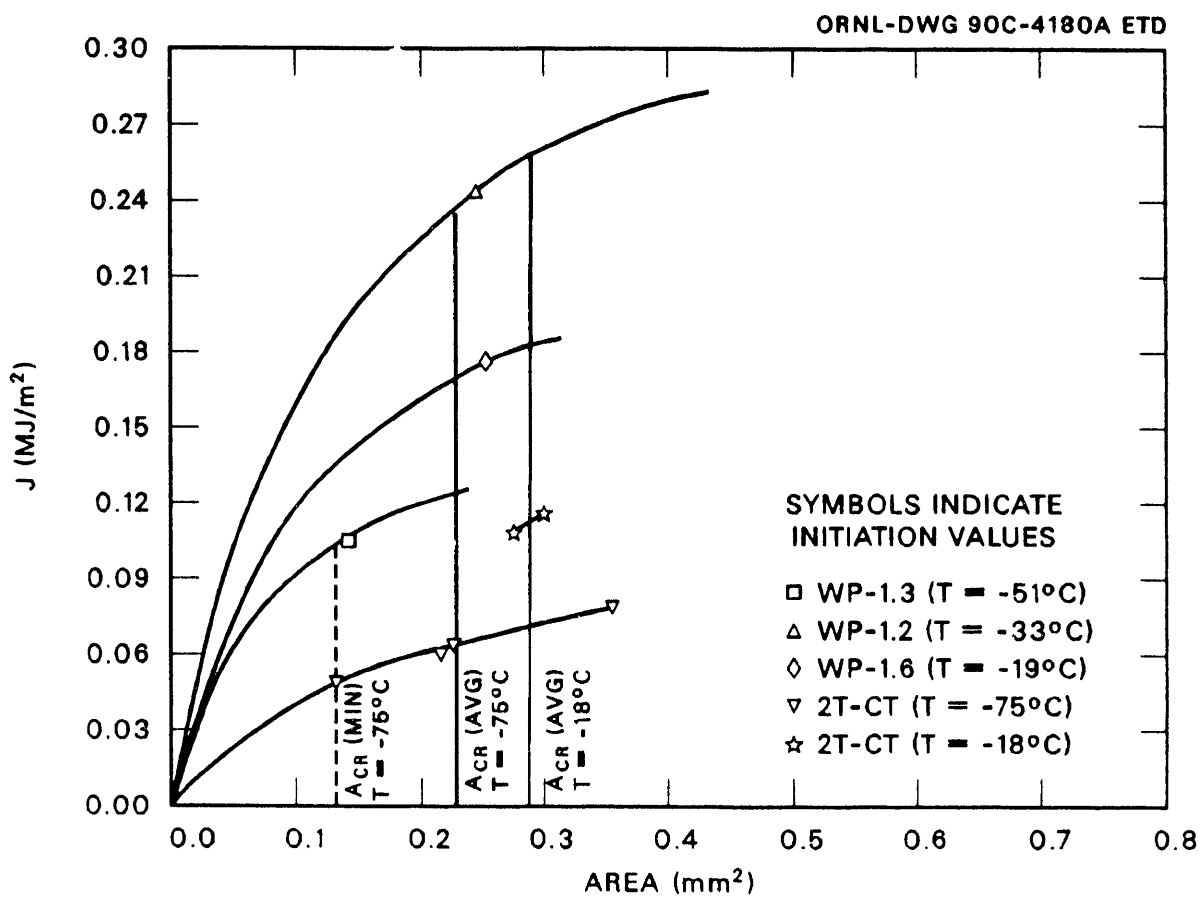

Fig. 15. J-integral values vs critical area within a critical stress contour of 1400 MPa in the 2T-CT and WP specimens.

components for the chevroned wide plate. The initiation J value was successfully predicted for WP-1.6. The area achieved by WP-1.3 at initiation fell short of the average CT value of –75°C but was above the minimum A_{CR} value.

Critical areas within the σ_{p1} = 1400 MPa contour from the 3-D analyses of the 1T-CT specimen and WP-1.2 cannot be reconciled with the corresponding 2-D analysis results. As described in the following section, this discrepancy is probably related to mesh refinement and numerical difficulties associated with the 3-D finite-element models used in the present study.

5.3 DISCUSSION OF RESULTS

Based upon the analysis results presented in this section, several observations can be made concerning the interpretations of local crack-tip fields using the fracture correlation parameters described in the previous section. To begin with, comparisons of hydrostatic constraint factors computed from both the 2-D and 3-D analyses of CT and WP specimens indicate that constraint at the midplane is lower for the WP specimen but still in the plane-strain range (see, for example, Fig. 12). Furthermore, the average constraint factor for both the CT and WP geometries varies only moderately over the range of applied loads considered in the analyses (see Fig. 14). Consequently, partly because of this relative insensitivity to loading, it was not possible to use hydrostatic constraint as a parameter to correlate J values at initiation in these geometries. The maximum principal stress criterion based on achieving a critical area within a selected stress contour appears to offer promise for interpreting cleavage initiation in terms of local crack-tip fields. The 2-D analyses of the 2T-CT specimens at –75°C and at –18°C provide contour areas corresponding to initiation that are consistent with the values calculated from the 2-D model of WP-1.2 and WP-1.6. It is probable that these estimates could be further refined with analyses based on improved modeling of the crack-tip zone.

Critical areas calculated from the 3-D models of the CT and WP specimens cannot presently be reconciled with the 2-D analysis results. Apparently, the difficulties stem from lack of sufficient mesh refinement in the crack-tip area. It can be observed in Fig. 16 (from Ref. 17) that the contour for σ_1/σ_o = 3.2 extends approximately 0.148 mm from the crack plane. The 3-D model for the WP specimen shown in Fig. 17, at the time of initiation, has a contour for σ_{p1} = 1460 MPa contained just in the first ring of elements to the right of the crack tip (an element length of 0.75 mm). This severely limits an accurate volume or area calculation. Clearly, if constraint conditions are to be incorporated through 3-D modeling of the crack-tip region, then greater mesh refinement will be required to achieve accurate representation of the local crack-tip fields.

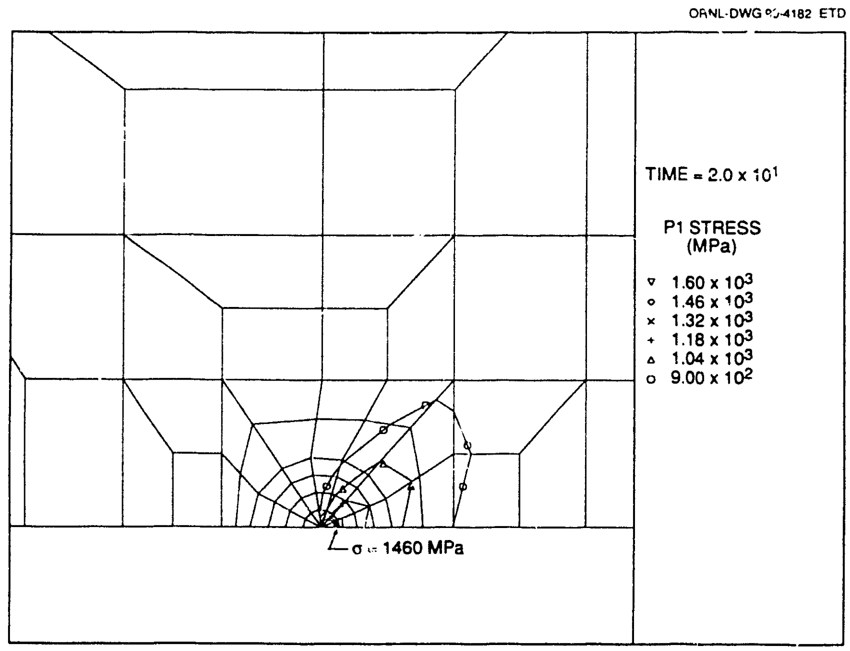

Fig. 17. Principal stress contours at the initiation load of 18.9 MN for the wide-plate specimen WP-1.2.

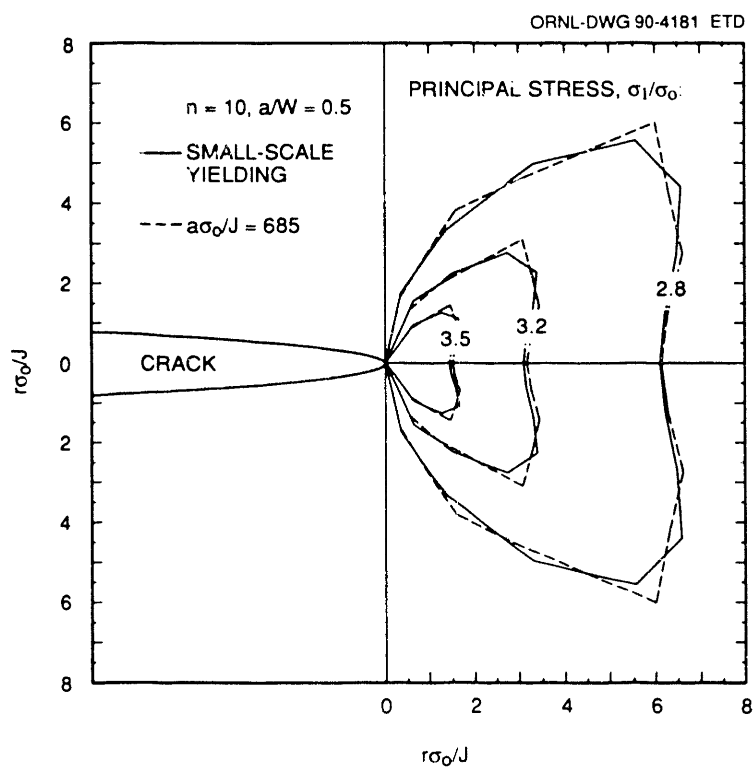

Fig. 16. Comparison of principal stress contours in small-scale yielding and in an SENB specimen for a/W = 0.5 and hardening exponent of n = 10. *Source*: R. H. Dodds, Jr., and R. L. Anderson, *A Framework to Correlate a/W Ratio Effects on Elastic-Plastic Fracture Toughness (Jc)*, Report UILU-ENG-90-2002, University of Illinois, Champaign, Illinois, January 1990.

6. SUMMARY AND CONCLUSIONS

Elastic-plastic 2-D and 3-D finite-element analyses of CT and WP specimens of A 533 B steel were carried out to correlate a selected local crack-tip parameter with measured cleavage initiation loads. Results of the study can be summarized as follows:

1. Comparisons of the hydrostatic constraint factor evaluated from the CT and WP specimen solutions indicate that midplane constraint is lower for the WP specimen and varies only moderately over the range of applied loads for both geometries. It was not possible to use the hydrostatic constraint as a factor to correlate J values at initiation in the two geometries because of the insensitivity of h to loading.
2. The maximum principal stress criterion based on achieving a critical area within a selected principal stress contour successfully correlated the cleavage initiation toughness values for wide-plate tests WP-1.2 and WP-1.6 with measured toughness values from the 2T-CT specimen tests. By plotting applied J values for the small and large specimens vs the area within a critical stress contour, one can predict the initiation J for the large specimen from the critical areas attained by the small specimens at initiation. In effect, these areas and J values are used as a two-parameter model for predicting cleavage initiation in the larger structure. These results were obtained using 2-D plane-strain analyses of the two-specimen geometries. It is anticipated that further improvement in the correlation is possible with more refined finite-element models.
3. Analysis results from the 3-D models of the CT and WP specimens cannot presently be reconciled with the 2-D analysis results. Clearly, these difficulties stem from lack of sufficient mesh refinement (both in-plane and through-thickness) in the crack-tip region of the 3-D models.

Results from this study indicate that future focus should be on detailed 2-D plane-strain elastic-plastic analyses of the CT and WP geometries. It was observed that important results can be obtained from 2-D analyses without the excessive computing resource requirements of 3-D analyses. Highly refined meshes at the crack tip are required to accurately compute the enclosed areas for the maximum principal stress criterion. Based on values of cumulative area and applied J, the two-parameter model should be tested further to establish its transferability between laboratory specimens and engineering structures for predicting cleavage initiation.

7. REFERENCES

1. D. J. Naus et al., Martin Marietta Energy Systems, Inc., Oak Ridge Natl. Lab., *Crack-Arrest Behavior in SEN Wide Plates of Quenched and Tempered A533 Grade B Steel Tested Under Non-Isothermal Conditions*, USNRC Report NUREG/CR-4930 (ORNL-6338), August 1987.*

2. J. G. Merkle, Martin Marietta Energy Systems, Inc., Oak Ridge Natl. Lab., *An Examination of the Size Effects and Data Scatter Observed in Small-Specimen Cleavage Fracture Toughness Testing*, USNRC Report NUREG/CR-3672 (ORNL/TM-9088), April 1984.*

3. D. J. Naus et al., Martin Marietta Energy Systems, Inc., Oak Ridge Natl. Lab., "Summary of HSST Wide-Plate Crack-Arrest Tests and Analyses," pp. 17–40 in *Proceedings of United States Nuclear Regulatory Commission Fifteenth Water Reactor Safety Information Meeting*, USNRC Conference Proceeding NUREG/CP-0091, Vol. 2, February 1988.*

4. D. J. Naus et al., Martin Marietta Energy Systems, Inc., Oak Ridge Natl. Lab., "HSST Wide-Plate Test Results and Analysis," pp. 291–317 in *Proceedings of United States Nuclear Regulatory Commission Sixteenth Water Reactor Safety Information Meeting*, USNRC Conference Proceeding NUREG/CP-0097, Vol. 2, March 1989.*

5. D. J. Naus et al., Martin Marietta Energy Systems, Inc., Oak Ridge Natl. Lab., "High Temperature Crack-Arrest Behavior of Prototypical and Degraded (Simulated) Reactor Pressure Vessel Steels," *Int. J. Pressure Vessels & Piping* **39**, 189–208 (1989).†

6. D. J. Naus et al., Martin Marietta Energy Systems, Inc., Oak Ridge Natl. Lab., *High-Temperature Crack-Arrest Behavior in 152-mm-Thick SEN Wide Plates of Quenched and Tempered A533 Grade B Class 1 Steel*, USNRC Report NUREG/CR-5330 (ORNL/TM-11083), April 1989.*

7. C. E. Pugh et al., Martin Marietta Energy Systems, Inc., Oak Ridge Natl. Lab., "Crack Run-Arrest Behavior in Wide SEN Plates of a LWR Pressure Vessel Material," Paper G1/4, pp. 21–26 in *Transactions of the 9th International Conference on Structural Mechanics in Reactor Technology*, American Association for Structural Mechanics in Reactor Technology, 1987.

8. G. R. Irwin, University of Maryland, "The Effect of Size Upon Fracturing," pp. 176–194 in *Symposium on Effect of Temperature on the Brittle Behavior of Materials with Particular Reference to Low Temperatures*, ASTM STP 158, American Society for Testing and Materials, 1954.

9. G. R. Irwin, University of Maryland, "Fracture Mode Transition for a Crack Traversing a Plate," *J. Basic Eng.* **82**(2), 415–425 (1960).†

10. H. G. Pisarski, "Influence of Thickness on Critical Crack Opening Displacement (COD) and J Values," *Int. J. Fract.* **18**(4), 427–440 (August 1981).†

11. G. G. Chell and D. A. Curry, "Mechanics and Mechanisms of Cleavage Fracture," Chap. 3 in *Developments in Fracture Mechanics—2nd Edition*, G. G. Chell, Applied Science Publishers, London, 1981.

12. J. D. Landes and D. H. Shaffer, "Statistical Characterization of Fracture in the Transition Region," pp. 368–382 in *Fracture Mechanics: Twelfth Conference*, ASTM STP 700, American Society for Testing and Materials, 1980.

13. W. R. Andrews, V. Kumar, and M. M. Little, "Small-Specimen Brittle-Fracture Toughness Testing," pp. 476–598 in *Fracture Mechanics: Thirteenth Conference*, ASTM STP 743, American Society for Testing and Materials, 1981.

14. A. R. Rosenfield and D. K. Shetty, "Cleavage Fracture in Steel in the Ductile-Brittle Transition Region," pp. 196–209 in *Elastic-Plastic Fracture Test Methods: The Users' Experience,* ASTM STP 856, American Society for Testing and Materials, 1985.

15. R. O. Ritchie, J. F. Knott, and J. R. Rice, "On the Relationship Between Critical Tensile Stress and Fracture Toughness in Mild Steel," *J. Mech. Phys. Solids* **21**, 395–410 (1973).†

16. T. L. Anderson and R. H. Dodds, Jr., *Specimen-Size Requirements for Fracture Toughness Testing in the Transition Region*, Report MM-6586-90-5, Texas A&M University, College Station, Texas, Mechanics and Materials Center, May 1990.

17. R. H. Dodds, Jr., and T. L. Anderson, *A Framework to Correlate a/W Ratio Effects on Elastic-Plastic Fracture Toughness (Jc),* Report UILU-ENG-90-2002, University of Illinois, Champaign, Illinois, January 1990.

18. M. F. Kanninen, and C. H. Popelar, *Advanced Fracture Mechanics*, Oxford University Press, New York, 1985.

19. J. R. Rice and D. M. Tracey, "On the Ductile Enlargement of Voids in Triaxial Stress Fields," *J. Mech. Phys. Solids* **17**, 201–217 (1969).†

20. R. M. McMeeking, "Finite Deformation Analysis of Crack-Tip Opening Elastic-Plastic Materials and Implications for Fracture," *J. Mech. Phys. Solids* **26**, 357–381 (1977).†

21. R. M. McMeeking and D. M. Parks, "On the Criteria for J-Dominance of Crack-Tip Fields in Large-Scale Yielding," pp. 175–197 in *Elastic-Plastic Fracture*, ASTM STP 668, American Society for Testing and Materials, 1979.

22. H. Kordisch, E. Sommer, and W. Schmitt, "The Influence of Triaxility on Stable Crack Growth," *Nucl. Eng. Des.* **112**, 27–35 (1989).†

23. G. T. Hahn, A. Gilbert, and C. N. Reid, "Model for Crack Propagation in Steel," *J. Iron Steel Inst.* (London) **202**, 677–684 (August 1964).†

---

*Available for purchase from National Technical Information Service, Springfield, VA 22161.

†Available in public technical libraries.

NUREG/CR-5651
ORNL/TM-11692
Dist. Category RF

INTERNAL DISTRIBUTION

1. D. J. Alexander
2–4. B. R. Bass
5. S. H. Buechler
6–10. R. D. Cheverton
11. J. M. Corum
12. W. R. Corwin
13. J. S. Crowell
14. T. L. Dickson
15. F. M. Haggag
16. J. E. Jones Jr.
17. S. K. Iskander
18–20. J. Keeney-Walker
21. D. E. McCabe
22. J. G. Merkle
23. R. K. Nanstad
24. D. J. Naus
25–30. W. E. Pennell
31. C. E. Pugh
32. G. C. Robinson
33. D. K. Shum
34. T. J. Theiss
35. G. E. Whitesides
36. ORNL Patent Section
37. Central Research Library
38. Document Reference Section
39–40. Laboratory Records Department
41. Laboratory Records (RC)

EXTERNAL DISTRIBUTION

42. C. Z. Serpan, Division of Engineering, U.S. Nuclear Regulatory Commission, Washington, DC 20555
43–44. M. E. Mayfield, Division of Engineering, U.S. Nuclear Regulatory Commission, Washington, DC 20555
45. A. Taboada, Division of Engineering, U.S. Nuclear Regulatory Commission, Washington, DC 20555
46. R. H. Dodds, University of Illinois, Urbana, IL 61801
47. R. J. Dexter, Southwest Research Institute, San Antonio, TX 78284
48. R. F. Fields, National Institute of Standards, Gaithersburg, MD 20899
49. W. L. Fourney, Department of Mechanical Engineering, University of Maryland, College Park, MD 20742
50. E. M. Hackett, David Taylor Research Center, Annapolis, MD 21402
51. G. R. Irwin, Department of Mechanical Engineering, University of Maryland, College Park, MD 20742
52–54. J. D. Landes, University of Tennessee, Knoxville, TN 37996-2030
55. P. O'Donoghue, Dept. of Civil Engineering, University College Dublin, Earl Fort Terrace, Dublin, Ireland 2
56. C. W. Schwartz, Department of Mechanical Engineering, University of Maryland, College Park, MD 20742
57. E. T. Wessel, 312 Wolverine, Haines City, FL 33844
58. Office of Assistant Manager for Energy Research and Development, Department of Energy, Oak Ridge Operations, Oak Ridge, TN 37831

NRC FORM 335
(2-89)
NRCM 1102,
3201, 3202

U.S. NUCLEAR REGULATORY COMMISSION

BIBLIOGRAPHIC DATA SHEET

(See instructions on the reverse)

1. REPORT NUMBER
(Assigned by NRC. Add Vol., Supp., Rev., and Addendum Numbers, if any.)

NUREG/CR-5651
ORNL/TM-11692

2. TITLE AND SUBTITLE

An Investigation of Crack-Tip Stress Field Criteria for Predicting Cleavage-Crack Initiation

3. DATE REPORT PUBLISHED

MONTH	YEAR
September	1991

4. FIN OR GRANT NUMBER

B0119

5. AUTHOR(S)

J. Keeney-Walker, B. R. Bass, and J. D. Landes

6. TYPE OF REPORT

Technical

7. PERIOD COVERED *(Inclusive Dates)*

8. PERFORMING ORGANIZATION – NAME AND ADDRESS *(If NRC, provide Division, Office or Region, U.S. Nuclear Regulatory Commission, and mailing address; if contractor, provide name and mailing address.)*

Oak Ridge National Laboratory
P. O. Box 2008
Oak Ridge, Tennessee 37831

9. SPONSORING ORGANIZATION – NAME AND ADDRESS *(If NRC, type "Same as above"; if contractor, provide NRC Division, Office or Region, U.S. Nuclear Regulatory Commission, and mailing address.)*

Division of Engineering
Office of Nuclear Regulatory Research
U. S. Nuclear Regulatory Commission
Washington, DC 20555

10. SUPPLEMENTARY NOTES

11. ABSTRACT *(200 words or less)*

Cleavage crack initiation in large-scale wide-plate (WP) specimens could not be accurately predicted from small, compact (CT) specimens utilizing a linear elastic fracture mechanics, K_{Ic}, methodology. In the wide-plate tests conducted by the Heavy-Section Steel Technology Program at Oak Ridge National Laboratory, crack initiation has consistently occurred at stress intensity (K_I) values ranging from two to four times those predicted by the CT specimens. The work centers around nonlinear two- and three-dimensional finite-element analyses of the crack-tip stress fields in these geometries. Analyses were conducted on CT and WP specimens for which cleavage initiation fracture had been measured in laboratory tests. The local crack-tip fields generated for these specimens were then used in the evaluation of fracture correlation parameters to augment the K_I parameter for predicting cleavage initiation. Parameters of hydrostatic constraint and of maximum principal stress, measured volumetrically, are included in these evaluations. The results suggest that the cleavage initiation process can be correlated with the local crack-tip fields via a maximum principal stress criterion based on achieving a critical area within a critical stress contour. This criterion has been successfully applied to correlate cleavage initiation in 2T-CT and WP specimen geometries.

12. KEY WORDS/DESCRIPTORS *(List words or phrases that will assist researchers in locating the report.)*

Cleavage-crack initiation	constitutive models	hydrostatic constraint
maximum principal stress	fracture mechanics	wide-plate
compact specimens	finite element analysis	fracture correlation parameters

13. AVAILABILITY STATEMENT

Unlimited

14. SECURITY CLASSIFICATION

(This Page)
Unclassified

(This Report)
Unclassified

15. NUMBER OF PAGES

16. PRICE

NRC FORM 335 (2-89)

END

DATE
FILMED

11 / 25 / 91